2014

FOLATE CONJUGATED DENDRIMERS FOR TARGETED ANTICANCER THERAPY

Shannon Andrews
Virginia Commonwealth University

© Shannon Andrews 2014

All Rights Reserved

FOLATE CONJUGATED DENDRIMERS FOR TARGETED ANTICANCER

THERAPY

A thesis submitted in partial fulfillment of the requirements for the degree of Master of Science at Virginia Commonwealth University School of Medicine.

by

SHANNON CHRISTINE ANDREWS
Bachelor of Science, Virginia Commonwealth University, December 2010
Post-Baccalaureate Certificate in Pre-Medical Graduate Health Sciences, VCU 2013

Director: W. ANDREW YEUDALL
ASSOCIATE PROFESSOR, DEPT OF ORAL & CRANIOFACIAL MOLECULAR
BIOLOGY, & DIRECTOR OF BASIC DENTAL SCIENCE EDUCATION, VCU

Virginia Commonwealth University
Richmond, Virginia
August 2014

Table of Contents

List of Figures

Abstract

FOLATE CONJUGATED DENDRIMERS FOR TARGETED ANTICANCER THERAPY

By Shannon Christine Andrews, Bachelor of Science

A thesis submitted in partial fulfillment of the requirements for the degree of Master of Science at Virginia Commonwealth University School of Medicine.

Virginia Commonwealth University, 2014

Major Director: W. Andrew Yeudall
ASSOCIATE PROFESSOR, DEPT OF ORAL & CRANIOFACIAL MOLECULAR BIOLOGY, & DIRECTOR OF BASIC DENTAL SCIENCE EDUCATION, VCU

Anticancer therapeutics are often limited to suboptimal doses due to their lack of selectivity for tumor cells and resultant damage to healthy tissue. These limitations motivated researchers to develop tumor-specific delivery systems for improved therapeutic efficacy and reduced unintended cytotoxicity. Polyamidoamine dendrimers offer an ideal platform for designing targeted therapeutics with tunable characteristics that optimize

pharmacokinetic behavior and targeting specificity[1]. Ligand conjugation to dendrimer provides the biochemical interaction necessary to activate tumor-specific receptors for receptor-mediated endocytosis and effective internalization of polyplexes[2]. Tumor-specific receptors overexpressed in carcinomas, like folate receptor-alpha (FOLRα), are targeted by ligand-conjugated dendrimer to allow enhanced internalization of dendrimer and its therapeutic cargo. We examined the cellular trafficking dynamics and potential of folate-conjugated dendrimer for nucleic acid delivery *in vitro.* Results show folate-conjugation to G4 PAMAM dendrimer (G4FA) confers enhanced uptake in FOLRα-positive tumor cells. Cells internalize G4FA in a receptor-dependent manner with specificity for FOLRα-positive tumor cells.

1. Introduction

1.1 Cancer Prevalence and Tumor Development

According to the American Cancer Society, one half of all men and one third of all women in the US will develop cancer during their lifetime. Cancer is a common term for over 100 disease types, marked by abnormal cellular growth, malignant behavior, tumor development, and eventually invasion and metastasis. It is among the leading causes of death worldwide, claiming over 8.2 million lives in 2012 alone[25]. Although incidence is high, overall cancer death rates are decreasing in the United States according to the 'Annual Report to the Nation on Cancer Status', conducted by a collaboration of the American Cancer Society, the Centers for Disease Control and Prevention (CDC), the National Cancer Institute (NCI), and the American Association of Central Cancer Registries (NAACCR)[3]. The decline in overall cancer morbidity reflects progress in cancer control and prevention, made possible through enhanced ability for early detection and improved treatment options. Uncovering the human genome allowed discovery of cellular and molecular mechanisms driven by human diseases. As the complex intricacies of human disease states are unraveled, in parallel with biotechnological advances, opportunity arises to improve diagnostics, prevention, and treatment options.

Carcinogenesis is a complex, multistep process involving numerous cellular physiological systems[2]. Cells become cancerous when genetic mutations accumulate and cause changes in normal cell behavior[2]. Genetic mutations of oncogenes and tumor

1

suppressor genes may result in uncontrolled cellular proliferation, amplified genomic disorganization, tumor development, and malignancy[4]. The inherent complexity of cancer, in its many varieties, implies a multifaceted, individualized treatment plan based on tumor type.

1.2 Gliomas

Of particular interest to this paper is the treatment of gliomas, which have a particularly dismal prognosis due to the disease state's highly invasive nature. Gliomas account for more than 70% of all brain tumors, including gliomas of astrocytic, oligodendroglial, and ependymal origin[5,6]. Glioblastoma multiforme (GBM) is the most malignant and most frequent glioma, accounting for 65% of gliomas[5,6]. Less than 3% of GBM patients are still alive five years post-diagnosis[6]. This poor prognosis reflects a major challenge associated with treatment of central nervous system (CNS) disease states. Disorders of the CNS possess peripheral barriers, like the blood-brain barrier (BBB), making it nearly impossible to penetrate with therapeutics. Approximately 98% of small-molecule drugs and all large molecule drugs fail to cross the BBB, aside from a few natural peptides and proteins, like insulin[1]. Therefore, it is essential to find ways to improve delivery of therapeutics to CNS in order to diminish the poor prognosis associated with such lethal disease states.

1.3 Anticancer Therapeutic Limitations and Potential Solutions

Currently, cancer treatment is based on clinical staging determined by morphologic diagnostics and therapeutic methods are limited to surgery, radiation, and chemotherapeutics[2]. These conventional methods aim to halt tumor progression, either by surgical removal or with ionizing radiation and/or chemically based chemotherapeutics which kill tumor cells through dramatic disruption of physiological pathways. Chemotherapeutics target components of cell cycle regulation active in proliferative cells to effectively arrest cellular growth and activate cell death pathways. This method effectively targets and destroys highly proliferative tumor cells, but it also damages healthy tissue that is proliferative under normal circumstances, like myelogenic or gastrointestinal cells, for example. This off target tissue damage gives rise to the side effects traditionally associated with anticancer therapeutics, including myelo- and immunosuppression, fatigue, alopecia, etc. and limits the use and efficacy of these drugs.

Anticancer therapeutics are often limited to suboptimal doses due to their lack of selectivity for tumor cells and resultant damage to healthy tissue. Dose limitation leads to inadequate drug concentrations at the tumor site, development of drug resistance, and treatment failure[2,7]. These limitations associated with standard treatment options have motivated researchers to develop targeting mechanisms intended to decrease off-target side effects and improve therapeutic efficacy. The central objective of targeted therapy is to direct therapeutics in sufficient quantities to the appropriate location.

3

1.4 Nanomedicine in Targeted Anticancer Therapeutics

The biomedical application of nanotechnology, i.e. nanomedicine, allows for incredible innovation in health care research to design and engineer highly advanced nano-scale devices that operate at the cellular and molecular level—precisely where many disease processes generate and perpetuate[2]. Nano-scale delivery systems, i.e. nanocarriers, including liposomes, nanoparticles, polymeric micelles, dendrimers, linear polymers, nanogels, etc. have received great attention in the development of targeted therapeutics due to their multifunctional nature and molecular level of action[2]. Their use as synthetic vectors for the delivery of gene therapy, imaging agents, antimicrobials, and chemotherapeutics has great potential to improve diagnostics and treatment of human disease processes[8]. Polymer- and nanoparticle-based delivery systems have been extensively reviewed and employed for medical diagnostics, imaging, and treatment[9]. Specific design of nanocarrier size, composition, solubility, electric charge, and chemical structure facilitates the delivery system's capabilities for specific use. These tunable characteristics can be selected for specific design in personalized treatment.

Recent approaches in anticancer therapy aim at enhancing vector specificity to improve therapeutic efficacy and reduce unintended cytotoxicity[7]. Nanoparticles can be targeted to specific sites via simple surface additions which provide the biochemical interaction with receptors expressed on target cells[2]. Tumor-specific molecular markers are targeted in order to direct therapy to tumor cells, and effectively bypass normal cells[10]. Research shows that the addition of a tumor-targeting mechanism, regardless of nanocarrier type, enhances internalization and therapeutic efficacy of the delivery system[9].

4

Folate receptor-alpha (FOLRα), a GPI anchored glycoprotein, is an attractive target for ligand-directed therapeutics due to its frequent overexpression in a variety of malignancies and little to no measurable expression in normal tissue[11]. Dendrimers, a class of macromolecules with highly branched 3D structure, are ideal nanocarriers for targeted delivery due to their low polydispersity and multi-functionality[12]. Their highly branched three-dimensional structure provides an ideal platform for an array of surface modifications designed to render efficient, biocompatible molecules for targeted therapy. We hypothesize that folic acid utilized as a targeting ligand will enhance dendrimer specificity and uptake in FOLRα-positive tumor cells.

1.5 Dendrimers

Dendrimers are a unique class of macromolecules characterized by a compactly layered, tree-like architecture with multiple active terminal groups centralized around an initiator core[12]. They are composed of individual dendrons that radiate from a central core; each layer of branching unit constitutes one complete generation (G), identified by number[13]. A series of controlled chemical additions produces highly organized polymers with consistent, incremental increase in size, molecular weight, and number of surface groups with increase in generation number[13]. Commercialization of PAMAM dendrimers by Dendritech (Midland, MI) has allowed for their extensive use in nano-medical studies; their unparalleled properties over traditional polymers have placed them at the forefront of this research[12]. As delivery systems, dendrimers possess several advantageous characteristics over other nanocarriers. These include (1) multifunctionality and targeting

5

ability, (2) enhanced pharmacokinetic behavior, (3) enhanced stability, solubility, and permeability of drugs, (4) improved delivery efficiency, and (5) reduced side effects by targeted delivery[1].

Of particular interest to our studies are full generation four (G4) polyamidoamine (PAMAM) dendrimers, which possess 64 primary amine terminal ends on their surface. A full generation PAMAM dendrimer is polycationic, expressing primary amine on the molecule's surface, whereas a half-generation PAMAM dendrimer is polyanionic, expressing carboxylic acids on the surface[1]. Numerous active terminal ends present on PAMAM dendrimer surfaces provide an ideal, versatile platform for design of highly specialized nanodevices with high loading capacity. Functional moieties currently under investigation in association with dendrimer-based delivery systems include genes, antisense oligonucleotides, peptides, low-molecular weight drugs and/or imaging agents, among others[12].
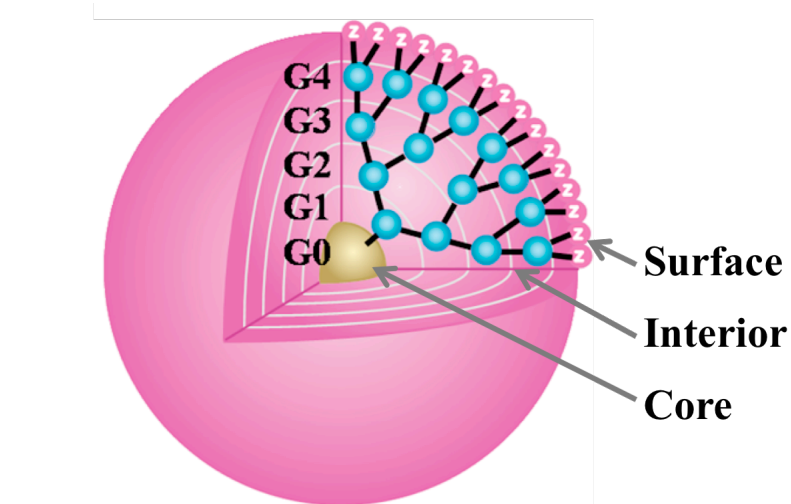
Figure 1. Generation Four Polyamidoamine Dendrimer. Schematic representation of

the structure of generation four PAMAM dendrimers. Abbreviations: G=generation;

Z=surface group for host-guest interactions and functionalization. Adapted from reference

1.[1]

Dendrimer-based delivery systems are capable of facilitating transport across cellular membranes and/or various biological barriers that often pose an issue with conventional delivery methods. Surface groups and molecular mass determine cellular entry dynamics of dendrimer-based delivery systems. Amine-terminated (cationic) dendrimers can efficiently complex with nucleic acids to form polyplexes that subsequently interact with negatively charged cell surface groups[12,14]. Tertiary amines present in the dendrimer branches provide high buffering capacity once polyplexes are internalized to endosomal vesicles. The dendrimer acts as a "proton sponge," wherein the amines enable adsorbtion of protons released from ATPase, causing osmotic swelling, effective endosomal escape, and release of polyplex into the cytoplasm[1,12,14]. Thus, the association of DNA with dendrimer allows efficient internalization of DNA; suggesting a viable approach for gene therapy and nucleic acid delivery, among several other potential pharmaceutical and biomedical applications of dendrimer-based delivery systems. Several studies suggest that favorable drug pharmacokinetics and high efficacy have been achieved using dendrimer nanocarriers[1].

Recent approaches aim at designing nanocarriers that possess specificity for diseased tissue in order to improve therapeutic efficacy and reduce off-target side effects. Active site-specific targeting of nanocarriers can be achieved by exploiting ligand-receptor relationships that induce receptor-mediated endocytosis of polyplexes. Receptors specifically overexpressed in diseased tissue, with little or no expression in normal tissue, provide a tumor-specific target to direct therapeutics. Ligand for the targeted receptor is conjugated to the nanocarrier surface to provide the biochemical interaction required to

8

activate the receptor and effectively internalize the dendrimer and its attached cargo[15]. Previous work in our lab has explored the use of EGF-conjugated dendrimers for receptor-mediated endocytosis through the EGFR receptor, which is overexpressed in many carcinomas. Results showed a 10-fold increase in gene delivery efficiency using the EGF-conjugated dendrimer as compared to dendrimer without ligand conjugation[14]. Exploration of similar pathways of receptor-mediated endocytosis merits further study in the design of targeted therapeutics to engineer efficient, biocompatible vectors with ideal biodistribution and pharmacokinetic behavior.

1.6 Folic Acid and FOLRα

Folic acid (FA) is an essential vitamin, provided by diet, that is naturally used in its reduced and/or polyglutamated forms in DNA biosynthesis and methylation[16]. The major route for folate acquisition in non-malignant cells is through the reduced folate carrier (RFC). This ubiquitously expressed anion channel has relatively low folate-binding affinity (K_m=1-10 µM) and will not internalize folate-conjugates[17]. Because folate is essential for the biosynthesis of nucleotide bases, it is consumed in elevated quantities in highly proliferative cells. To support their high folate demand, tumor cells frequently up-regulate expression of folate receptor-alpha (FOLRα; FOLR1), a GPI-anchored glycoprotein with very high affinity for folic acid (K_D~10^{-10} M)[18].

Among tumor targets/markers, FOLRα has many advantages for application in targeted therapeutics: (1) it binds folate, which is amenable to chemical conjugation with other molecules without affecting binding affinity[19], (2) FOLRα effectively internalizes

9

receptor-bound folate conjugates[20] (3) FOLRα expression is only found in measurable quantities in tumor cells and those involved in embryonic development (placenta, neural tubes) and folate resorption (kidney)[17]. High affinity of receptor for ligand-conjugates allows for administration of therapeutics at lower, less toxic concentrations, while still saturating available receptors to achieve the appropriate clinical response[21]. FOLRα is further identified as tumor-specific because its limited expression in normal tissue is confined to the apical surface of polarized epithelia[19]. Therefore, FOLRα expressed in normal tissue is unable to access intravenous FOLRα-directed therapeutics. However, upon malignant transformation, cell polarity is often lost in diseased epithelia and FOLRα becomes accessible to targeted drugs in circulation[11]. This dual mechanism for tumor-specificity has nominated the receptor's natural ligand, folic acid, as an attractive targeting ligand for therapies directed at FOLRα-positive malignancies[11]. Furthermore, folate is stable, small in size, it is compatible with a variety of solvents, and has high binding affinity for FOLRα, even when conjugated to other molecules ($K_D \sim 10^{-10}$ M)[11].

Several folate-conjugated nanoparticles are under investigation for targeted drug delivery and/or imaging; including metallic nanoparticles, micelles, mesoporous silica, liposomes, dendrimers, and nanotubes, among others[15]. Folate conjugates have successfully delivered imaging and therapeutic agents in malignant cells in both animal tumor models and human cancer patients, with preferential uptake seen in FOLRα+ cells[11,15,20]. Studies show folate-conjugated delivery systems exert low toxicity and show increased efficacy and pharmacokinetic behavior in comparison to non-targeted dendrimers and free pharmaceutical agents when applied *in vitro* and *in vivo*[15].

10

Exploitation of the FA/FOLRα ligand-receptor relationship has great potential in the design of targeted therapies; its characterization utilizing the utmost biocompatible, efficient vectors deserves more attention.

1.7 Hypothesis and Aims of the Current Study

We hypothesize that folate-conjugation to G4 PAMAM dendrimer will enhance dendrimer specificity and uptake in FOLRα positive tumor cells.

1. Examine the potential of G4FA as vector for intracellular delivery

2. Explore the cellular internalization/ trafficking dynamics of our synthetic vector

3. Evaluate *in vitro* targeting specificity of folate-conjugated dendrimer

2. Materials and Methods

MATERIALS

2.1 Cell culture

HN12 are derived from a lymph node metastasis in a patient with primary squamous cell carcinoma of the tongue[14] . T98A and U87A cells were provided by Dr. Gewirtz's lab in Massey Cancer Center at Virginia Commonwealth University (Richmond, VA). U87 cells are an epithelial-like astrocytoma/glioblastoma cell line classified as a class IV cancer. T98 cells are a fibroblast-like glioblastoma multiforme cell line. Cells were cultured on plastic culture plates and/or sterile glass cover-slips in Dulbecco's modified Eagle's medium (DMEM, Life Technologies, Grand Island, NY) supplemented with 10% fetal bovine serum (FBS), 100 units/ml of penicillin, and 100 μg/ml of streptomycin (both from Thermo Fisher Scientific, Asheville, NC) at 37^oC in humid environment with 10% CO_2.

2.2 PAMAM Dendrimers

Generation 4.0 polyamidoamine dendrimers were purchased from Dendritech, Inc. Design (Midland, MI). Engineering and characterization of PAMAM dendrimer derivatives was performed/provided by Leyuan Xu (responsible for all synthesis and labeling of FA-conjugated dendrimer derivatives)

12

2.3 Plasmids and Transfection Reagents

EPS8pr-GFP plasmid (pEZX-PF02) purchased from GeneCopoeia (Rockville, MD) includes an EPS8 promoter region that drives expression of the reporter gene, green fluorescence protein (GFP). Label IT® Cy3™ Plasmid Delivery Control (red) and TransIT keratinocyte transfection reagent (referred to as TransIT) were purchased from Mirus Bio (Madison, WI). Turbofect transfection reageant (referred to as Turbo) was purchased from Thermo Scientific (Rockford, IL).

2.4 Antibodies

Antibodies that recognize GFP (rabbit mAb #2956P), Rab5 (C8B1, rabbit mAb #3547S), RCAS1 (rabbit Ab #6960S), and Caveolin-1 (rabbit Ab #3238S) were purchased from Cell Signaling Technology (Danvers, MA). Dylight-594 Anti-Rabbit IgG antibody (#7074S) was purchased from Vector Laboratories (Burlingame, CA). Anti-actin (sc-1616) antibody was purchased from Santa Cruz Biotechnology (Santa Cruz, CA). Horseradish peroxidase conjugated rabbit anti-goat secondary antibody and HRP-linked anti-rabbit IgG antibody (#7074S) were purchased from Cell Signaling Technology (Danvers, MA). Western Lightning ECL was purchased from Perkin Elmer (Waltham, MA). DAPI

2.5 siRNA

esiRNA (endoribonuclease-prepared small interfering RNA) targeting Folate Receptor-α (siFOLRα), MISSION ® siRNA Universal Negative Control #1 (siNEG), and siRNA

13

targeting green fluorescent protein (siGFP), were purchased from Sigma-Aldrich (St. Louis, MO).

METHODS

2.6 qRT-PCR

Total RNA was extracted using Trizol reagent after washing with cold PBS twice. 3 μg of total RNA was reverse transcribed (Multiscribe[TM] Reverse Transcriptase, lot #1207114, Applied Biosystems, Life Technologies, Grand Island, NY) according to manufacturer's protocol. Real-time quantitative PCR was performed using ABI 7500 Fast System (Applied Biosystems, Rockville, MD) with fluorescence signal detection (SYBR-Green) after each cycle of amplification as previously described. The calculated cDNA copy number in each sample was derived from an extrapolated crossing point of a mathematically derived line extending from the exponential phase of amplification in a plot of fluorescence intensity (SYBR green) *versus* cycle number. For each reaction, diluted amounts of known templates provided quantitative standard curve reactions from which cDNA copy number could be determined. Tubulin was used as a housekeeping gene to normalize initial content of total cDNA in the samples. Oligonucleotide primers were designed using Primerbank database.

2.7 Fluorescence Microscopy:

Fluorescent images were taken using a Zeiss Axiovert 200 inverted fluorescence microscope (Carl Zeiss Microimaging, Thornwood, NY). Confocal microscopy was

14

performed at the VCU Dept. of Neurobiology & Anatomy Microscopy Facility, supported, in part, with funding from NIH-NIND Center core grant 5P30NS047463. Confocal images were taken using a Zeiss LSM 700 confocal laser scanning microscope (Carl Zeiss Microimaging, Thornwood, NY).

2.8 In vitro Transfection With EPS8pr-GFP plasmid

$1x10^4$ cells/well (T98A or U87A) were seeded on sterile, glass coverslips in 12-well plate and allowed to grow in 1 ml of growth medium containing 10% FBS for 24h. Cells were transfected via nucleofection (per manufacturer's protocol) or with the polyplexes of G4FA/pEPS8pr-GFP (20, 5, 1 μg/1 μg), or TransIT/pEPS8pr-GFP (5 μl/μg) suspended in 100 μl of growth medium containing 1% FBS. After 14h incubation at 37^oC and 10% CO_2, the medium in each well was replaced with fresh 1 ml growth medium containing 10% FBS. Cells were further incubated for 24h and then fixed in cold 100% methanol, counterstained for DAPI (1:2000 in 1xTBS), mounted in mounting medium (Vectashield, Vector Laboratories, Burlingame, CA) and studied under fluorescent microscopy.

Separate Transfection for Trypan Blue Assay: $5x10^4$ cells/well were seeded on sterile, glass coverslips in 12-well plate and allowed to grow in 1 ml of growth medium containing 10% FBS for 24h. Cells were transfected with the polyplexes of G4FA/pEPS8pr-GFP (20, 5, 1 μg/1μg) or Turbo/pEPS8pr-GFP (2 μl/1μg) suspended in 100 μl of growth medium containing 10% FBS. Diluted dendrimer/DNA mixture was added to each well (or left untreated for negative

15

control) rocked, and allowed to incubate at 37° C and 10% CO_2 for 48h before

trypan blue assay was conducted.

2.9 Trypan Blue Dye Exclusion Assay

48h post-transfection described above, wells were washed twice with 1xPBS, 300 μl of

0.1% trypsin was added per well and cells were recovered with 200 μl of growth medium.

Cells were spun at 4° for 5 minutes at 13000g. Cell pellets were resuspended in 100 μl of

1xPBS. 50μl of cell suspension was added to 50μl of 0.2% Trypan Blue in triplicate for

each experimental parameter and dye exclusion assay was performed in the Nexcelcom

AutoT4 cell counter according to the manufacturer's protocol.

2.10 *In vitro* Intracellular Trafficking Studies:

Co-localization of FITC-labeled Dendrimer With Cellular Organelle Protein Markers

$5x10^4$ cells/well were seeded on sterile, glass coverslips in 12 well plate and allowed to

grow in 1 ml of growth medium containing 10% FBS for 24 hours to allow for attachment.

Media was replaced in all wells with 1 ml fresh growth medium 24 hours after seeding.

Experimental wells were incubated with 5 μg of G4FA-FITC in 100 μl of growth medium,

added dropwise for various lengths of time (24 hr, 6h, 3h, 1h, 30 mins), rocked and

incubated at 37° C, 10% CO_2 until fixed in cold methanol for 15 minutes, air dried, and

stored -80° C until removed for staining and visualization under fluorescent microscopy.

Immunostaining of Cultured Cells:

16

Cells stored at -80° C were washed twice with 1xTBS, and blocked in 1.5% normal
goat serum (or 3% BSA) in TBS for 1 hour, covered, at ambient temperature.
Experimental wells were then incubated with monoclonal anti-Rab5 antibody
(Sigma) diluted 1:200, or anti-RCAS1 (1:800), or anti-CAV1 (1:500) in blocking
buffer overnight at 4°C (negative control wells were left in blocking buffer
overnight). All wells were washed three times with TBS, and incubated with
Dylight 594-conjugated anti-rabbit antibody (1:5000) and DAPI (1:1000) for 1
hour at ambient temperature. Cells were washed four times with TBS, 10 minutes
each on a shaker, and then mounted in Vectashield mounting media (Vector
Laboratories, Burlingame, CA) and imaged using a Zeiss Axiovert 200 microscope.

2.11 *In vitro* Trafficking of Plasmid DNA Delivered by G4FA

G4FA was labeled with fluorescein isothiocyanate (FITC). T98A cells were seeded on
glass coverslips in 12-well plate at density of $5x10^4$ cells/ well and allowed to grow in 1 ml
of growth medium containing 10% FBS for 24h. Cells were incubated with the polyplexes
of G4FA-FITC/LabelIT ™ Cy3^{TM} plasmid in 20:1 ratio (5μg/0.25 μg in 100 μl of growth
medium) for various lengths of time (30 min, 1h, 3h, 6h, 14h), fixed with cold methanol
for 10 minutes, counterstained with DAPI, and then rinsed with TBS buffer and mounted
for microscopy. Fluorescent images were taken under a Zeiss Axiovert 200 inverted
fluorescence microscope (Carl Zeiss Microimaging, Inc., Thornwood, NY).

2.12 siRNA-Mediated Knockdown of Folate Receptor-α

2×10^6 cells were transfected with 1 μg of either siFOLR1 or siNEG using the T-020 program of the Amaxa nucleofector (Amaxa biosystems). Cells were recovered in 20 ml of growth medium containing 10% FBS and plated into multiple wells: 1 ml/well was added directly to sterile, glass coverslips in 12-well plate (for treatment with nanovectors and imaging); and 3ml/ well were added to 6-well plates (for RNA isolation). 24h after transfection, one 6-well plate was snap frozen at 24h incubation point by aspirating media, washing in 1xPBS twice, parafilmed, and stored in -80^oC until taken out for RNA isolation 24h later. All other wells had media replaced with fresh growth medium containing 10% FBS and were allowed further incubation for 24 additional hours. 48h after nucleofection, RNA was isolated and reverse transcribed following manufacturer's protocol. qRT-PCR was performed to confirm gene knockdown.

2.13 Challenging Knockdown Cells With G4FA-FITC

48h following transfection with siRNA as described above, media was aspirated from the 12-well plate, and 5 μg of dendrimer (G4FA-FITC) suspended in 1000 μl media was added per well, rocked, and allowed to incubate at 37° C, 10% CO_2 for 1h before fixation in 100% cold methanol. Negative wells were left untreated; media was replaced with fresh 1 ml of growth medium at time of treatment to experimental wells and were fixed in methanol with experimental wells. Cells were counterstained with DAPI (1:1000 in 1xPBS) for thirty minutes covered at ambient temperature, then washed and mounted on microscope slides in Vectashield mounting medium (Vector Laboratories, Burlingame,

18

CA). Fluorescent images were taken with Zeiss Axiovert 200 inverted fluorescent microscope

2.14 G4FA Delivery of siRNA

5×10^4 cells (T98A-YFP and U87A-YFP) were seeded in 12 well plates, 6 wells included glass coverslips for subsequent fluorescent imaging while the remaining 6 wells were seeded for parallel, subsequent protein isolation. Cells were allowed to attach in 1 ml of growth medium containing 10% FBS for 24 hours. Cells were then treated with polyplexes of G4FA/siRNA (siYFP or siNEG) in 20:1 ratio (5 μg/0.25 μg) per well, suspended in 100 μl growth medium. Cells were allowed to incubate with polyplexes for 48h before further experimentation. 48h following transfection, 6 wells were subjected to protein lysis and Western blot analysis as described below, and the remaining 6 wells were fixed in cold methanol, counterstained with DAPI, and mounted in Vectashield mounting medium (Vector Laboratories, Burlingame, CA) for fluorescent microscopy.

2.14.1 Western Blot

After the growth medium was removed, cells were washed twice with cold PBS, lysed on ice for 10 minutes using 50 μl of cell lysis buffer (20 mM HEPES, pH 7.5, 10 mM EGTA, pH8.0, 40mM β-glycerophosphate, 1% NP-40, 2.5 mM $MgCl_2$, 20 μg/ml aprotinin, 20 μg/ml leupeptin, 1 mM PMSF), scraped immediately, and transferred to microcentrifuge tubes. Supernatant was transferred to a fresh tube after 10 min of microcentrifugation at 10,000 g at 4 °C. Cleared lysates were quantified using Bradford

19

assay (BCA; Biorad, Hercules, CA), and equivalent amounts of protein were resolved by SDS-PAGE and then transferred to polyvinylidene difluoride (PVDF) membrane (Immobilon-P; Millipore, Billerica, MA). Membrane was blocked in 5% milk in TTBS (10 mM Tris-HCl, pH 7.6, 0.5% Tween-20, 150 mM NaCl) for 1 h at room temperature, and then incubated in primary antibody diluted (1:10000 for YFP, 1:5000 for actin) in blocking buffer overnight at 4 °C. After washing in TTBS, bound primary antibodies were detected using horseradish peroxidase conjugated secondary antibodies and Western Lightning Enhanced Chemiluminescence (ECL; Perkin-Elmer, Waltham, MA).

3. Results and Conclusions

3.1 FOLRα Is Overexpressed In Tumor Cells

FOLRα is considered a highly selective tumor marker due to its frequent over-expression in a variety of tumor types, including carcinomas of the ovaries (>90%), endometrium, breast, lung, bladder, pancreas, kidney, brain, and neuro-endocrine carcinomas[18,22]. As shown in Figure 2, quantitative reverse transcription-polymerase chain reaction (qRT-PCR) experiments indicate that GBM-derived T98A cells express higher levels of FOLRα compared to glioblastoma-derived U87A cells, providing suitable contrast of FOLRα-expressing cell lines for use in our studies. This observation was confirmed with multiple RNA samples from these cell lines, isolated at different times from fresh cells. FOLRα overexpression was also evident in HNSCC-derived HN12 cells, lending support to evidence that FOLRα is frequently overexpressed in a variety of tumor types.
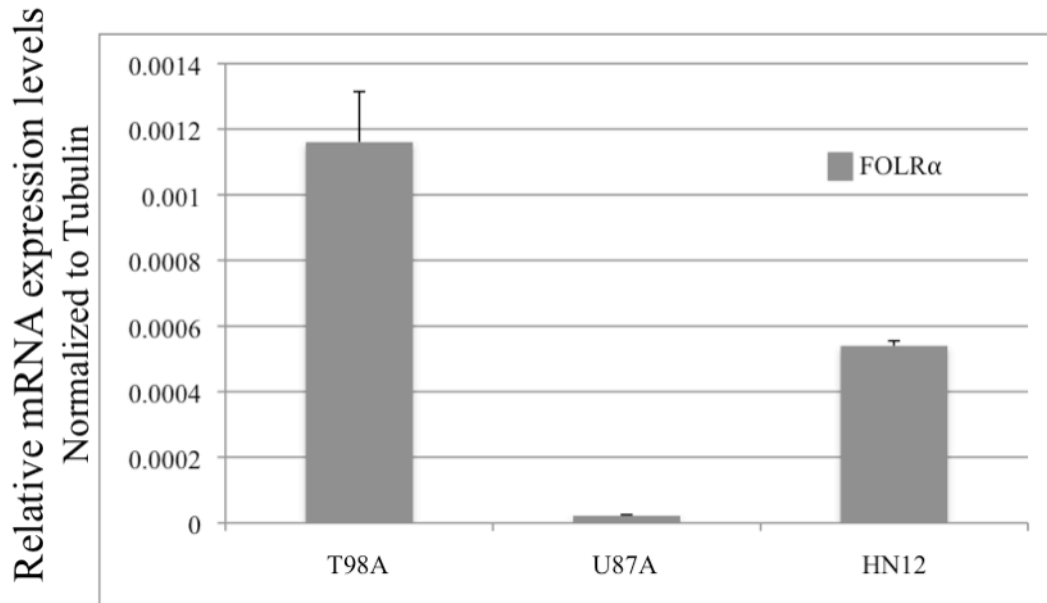
Figure 2. qRT-PCR: Folate Receptor Alpha. Folate Receptor-α (FOLRα) screen in T98A, U87A, HN12 cells. Total RNA was extracted, reverse-transcribed, and qRT-PCR performed. The relative expression ratio is defined as the expression levels of FOLRα to that of an internal standard, tubulin. Assays were carried out in triplicate; error bars represent SEM

22

3.2 G4-PAMAM Dendrimer Conjugated To Folic Acid (G4FA) Is An Effective Vector For Nucleic Acid Delivery

Gene therapy is a proven method for disease prevention and treatment, but efficient delivery systems are yet to be uncovered. Polyamidoamine (PAMAM) dendrimers readily form complexes with nucleic acids, including single-stranded oligonucleotides, circular plasmid DNA, linear RNA, and various sizes of double-stranded DNA[23], via electrostatic interaction between negatively charged phosphates of the nucleic acid and protonated primary amino groups on the dendrimer surface. A cationic surface charge is imparted to the complex through high dendrimer-DNA charge ratios, allowing subsequent interaction with the anionic glycoproteins and phospholipids residing on the cell membrane surface[23]. These interactions allow uptake of the DNA-dendrimer complex into the cell cytosol through passive transport or endocytosis[23]. The addition of a targeting moiety to dendrimer, prior to association with nucleic acid, should enhance the uptake of dendrimer-DNA complex through receptor-mediated endocytosis. We first wanted to explore the transfection capabilities of our folate-receptor targeted dendrimer at varying ratios with the delivery of plasmid DNA.

T98A and U87A cell lines were used to evaluate *in vitro* gene transfection efficiency of the folate-conjugated PAMAM dendrimer (G4FA) EPS8pr-GFP plasmid was delivered with G4FA at varying concentrations for comparison to standard transfection methods. The transfection efficiency was evaluated in terms of GFP expression, qualitatively illustrated by fluorescent images and quantified by counting cells expressing GFP, normalized with respect to the untreated control group. TransIT-keratinocyte

23

transfection reagent (referred to as TransIT) is a commercially available transfection reagent with high efficiency and low toxicity. Transfection of our plasmid induced cellular GFP expression, driven by the EPS8 gene promoter (epidermal growth factor receptor kinase substrate 8), which encodes proteins involved in actin cytoskeleton dynamics and the EGFR pathway. Reporter gene, GFP (enhanced green fluorescent protein), which fluoresces green when exposed to ultraviolet light, permitted visual confirmation of successful transfection.

Fluorescent images for each parameter are shown in Figure 3A and 3B for T98A and U87A cells, respectively. Fluorescence was detectable in all experimental parameters, excluding the untreated negative control, indicating that our PAMAM dendrimer conjugated to folic acid (G4FA) is capable of intracellular delivery of nucleic acids within 48 hours. Cytotoxicity was determined by averaging the cell count of multiple fields (n=10, ~10 cells/field= ~100 cells counted/parameter) for each parameter and relative cell viability was normalized with respect to the viability of the control group. Figure 3C indicates that increasing the molar concentration of delivery vector G4FA, with a constant amount of plasmid DNA, induces increased cell death to the overall cellular population in both cell lines. Transfection efficiency was quantified by averaging the percentage of cells expressing GFP, taken from multiple fields representative of the cell population for each experimental parameter. Our synthetic vector, G4FA, showed efficient transfection at all concentrations within both cell lines, although its highest concentration, at 20μg, permitted the highest success (Figure 3D/E).

24

Figure 3A: **Fluorescent Images Following EPS8pr-GFP Plasmid Transfection T98A.**
Analysis of GFP reporter gene expression in T98A cells following transfection with
EPS8pr-GFP plasmid DNA. Cells were cultured on glass coverslips for 24h and
transfected as described in 'Materials and Methods.' Cells were fixed in cold methanol,
counterstained with DAPI, and imaged under fluorescent microscopy. All images are
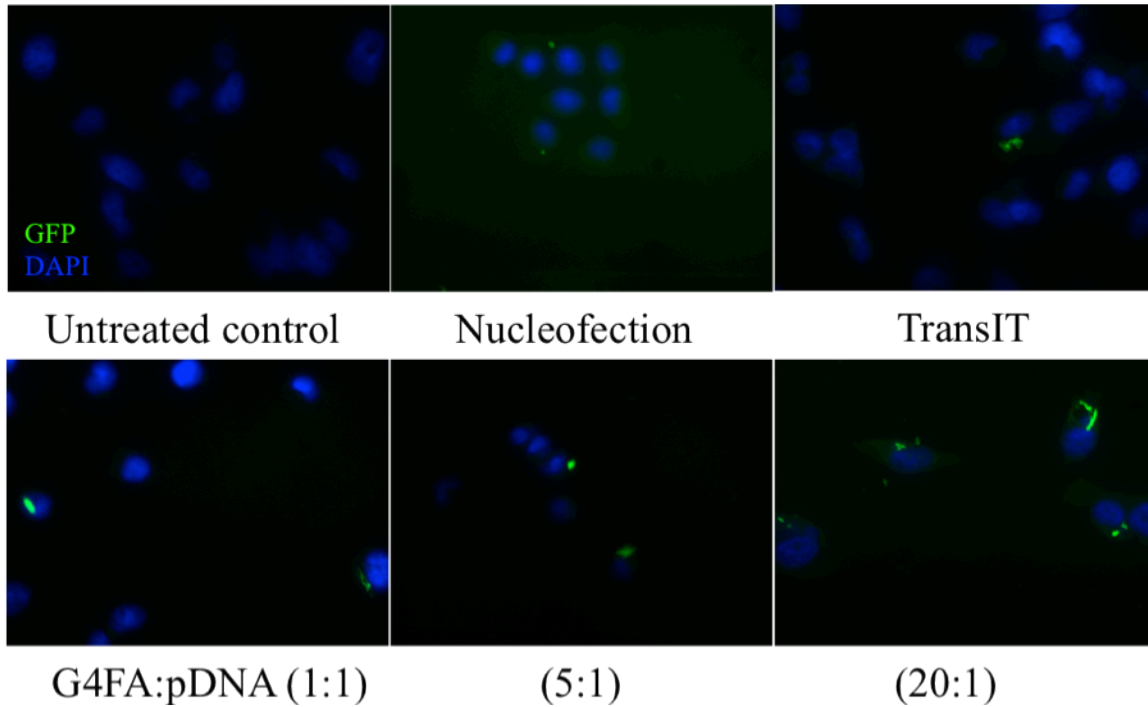viewed at 400x original magnification

25

Figure 3B: **Fluorescent Images Following EPS8pr-GFP Plasmid Transfection U87A**. Analysis of GFP reporter gene expression in U87A cells following transfection with EPS8pr-GFP plasmid DNA. Cells were cultured on glass coverslips for 24h and transfected as described in 'Materials and Methods.' Cells were fixed in cold methanol, counterstained with DAPI, and imaged under fluorescent microscopy. All images are viewed at 400x original magnification
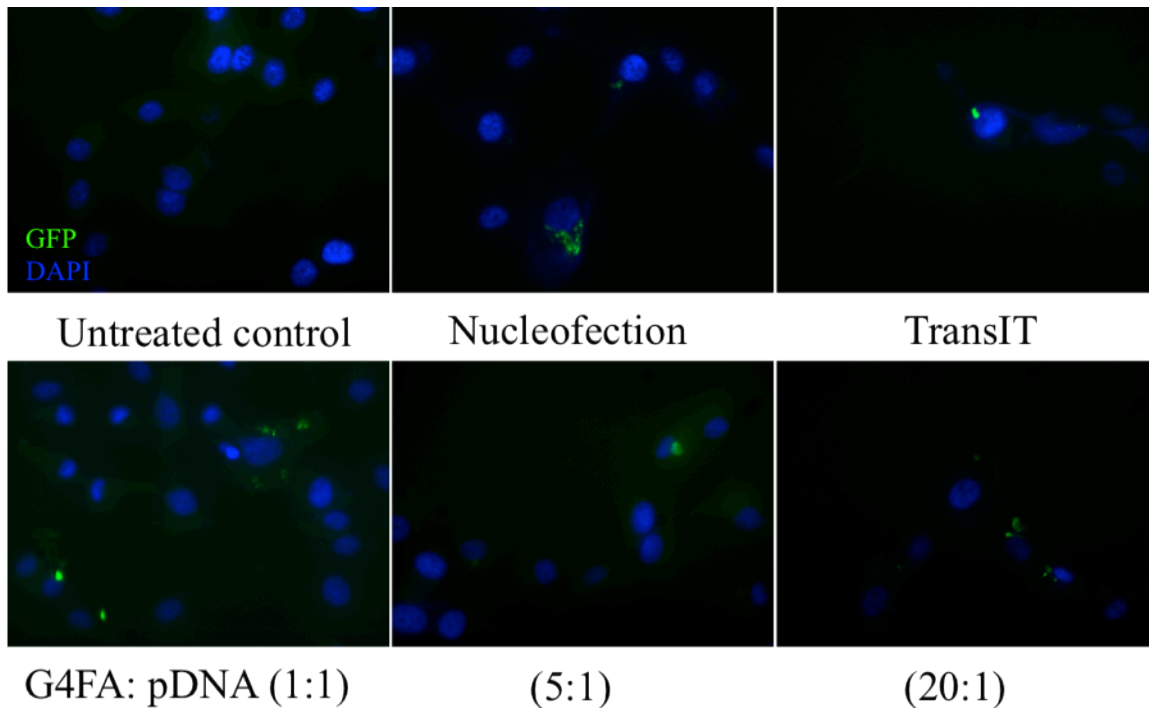
26

Cell Viability following Transfection
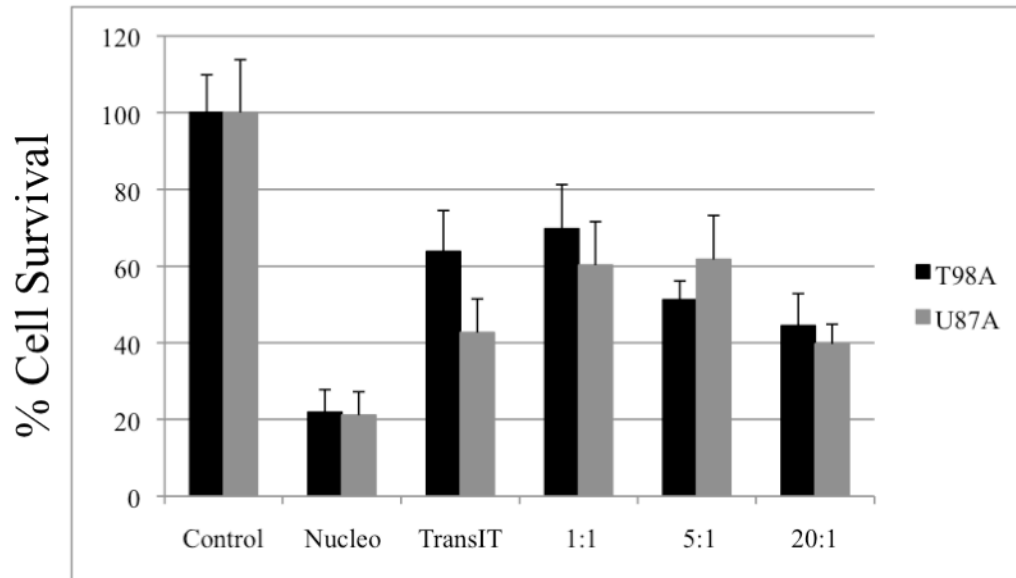
Figure 3C. Cell Viability Following Transfection in T98A and U87A Cells. Cell viability results in T98A and U87A cells following transfection with EPS8pr-GFP plasmid DNA via nucleofection (per manufacturer's protocol) or with the polyplexes of TransIT/pEPS8pr-GFP (5 μl/μg) or folate conjugated dendrimer (G4-FA)/pEPS8pr-GFP at varying concentrations (20, 5, 1 μg/1 μg), as described in 'Materials and Methods' section. Control=untreated, Nucleo= nucleofected, TransIT= keratinocyte transfection reagent, 1:1, 5:1, 20:1= G4FA:EPS8pr-GFP (ug). Cytotoxicity was quantified by counting cells in ten fields per parameter in each cell line. Average cell number for ten fields was calculated and normalized with respect to the viability (cell number) of the control group. Error bars represent standard deviation in samples for each cell line.

27

Figure 3D. Transfection Efficiency T98A. Transfection efficiency in T98A cells using folate-conjugated dendrimer (G4FA/pDNA) at varying concentrations (20, 5, 1 μg/1 μg) to deliver EPS8pr-GFP plasmid DNA as compared to standard transfection methods, as described in Methods section. Control=untreated, Nucleo= nucleofected, TransIT= keratinocyte transfection reagent, 1:1, 5:1, 20:1= G4FA:EPS8pr-GFP (ug).

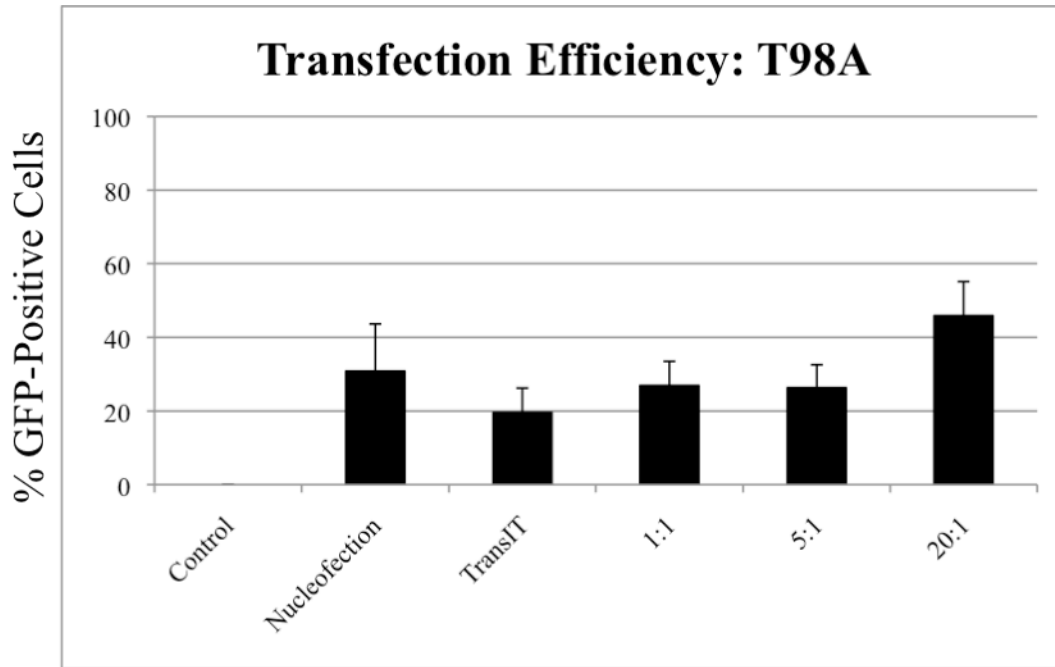**Figure 3E. Transfection Efficiency U87A.** Transfection efficiency in U87A cells using folate conjugated dendrimer (G4FA/pDNA) at varying concentrations (20, 5, 1 μg/1 μg) to deliver EPS8pr-GFP plasmid DNA as compared to standard transfection methods described in the Methods section. Control=untreated, Nucleofection= nucleofected, TransIT= keratinocyte transfection reagent, 1:1, 5:1, 20:1= G4FA:EPS8pr-GFP (ug).
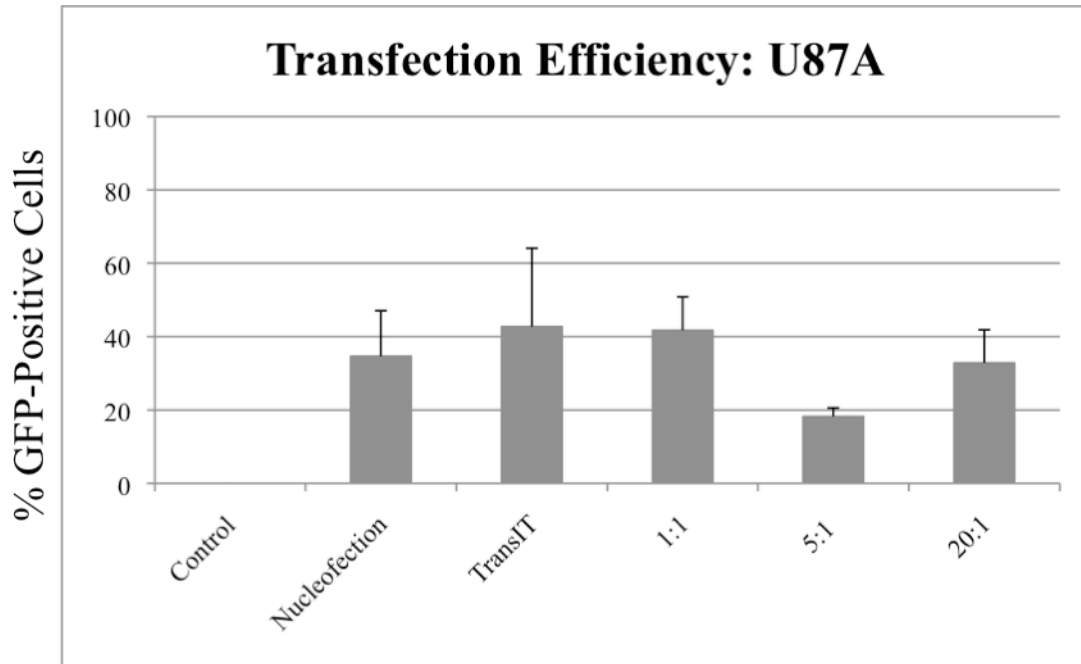
3.3 G4FA:EPS8pr-GFP Complex Conveys High Transfection Efficiency With Limited Cytotoxicity

In vitro transfection implies a trade-off between transfection efficiency and cell viability. Delivery systems with high transfection efficiency also tend to exert high cytotoxicity. We wanted to explore cell viability with a universal viability assay following transfection of cells with folate-conjugated dendrimer complexed with plasmid DNA. Trypan Blue viability assay is a dye exclusion method that utilizes membrane integrity to identify dead cells. Dead cells will stain blue because their compromised cellular membrane allows uptake of the trypan blue dye. These cells are identified by cellometer software with bright field imaging using Nexcelcom Cellometer AutoT4 Cell counter (Bioscience LLC, Lawrence, MA).

Trypan blue assay was conducted in triplicate for each experimental parameter including dendrimer/DNA complexed at varying ratios (20, 5, 1μg/1μg) or turbofection using turbo/EPS8pr-GFP (2μl/1μg) and negative, untreated control for each cell line. Results in Figure 4 show a general trend of increased cytotoxicity as dendrimer concentration is increased, supporting earlier results (Figure 3C) of cell viability with the same parameters. Taken together with the transfection efficiency results in figures 3D/E, it is apparent that increased transfection efficiency causes decreased cell viability, but differences are small when using our synthetic vector. These results demonstrate that our folate-conjugated dendrimer is a viable approach for efficient delivery of nucleic acids with limited cytotoxicity, even at higher concentrations.

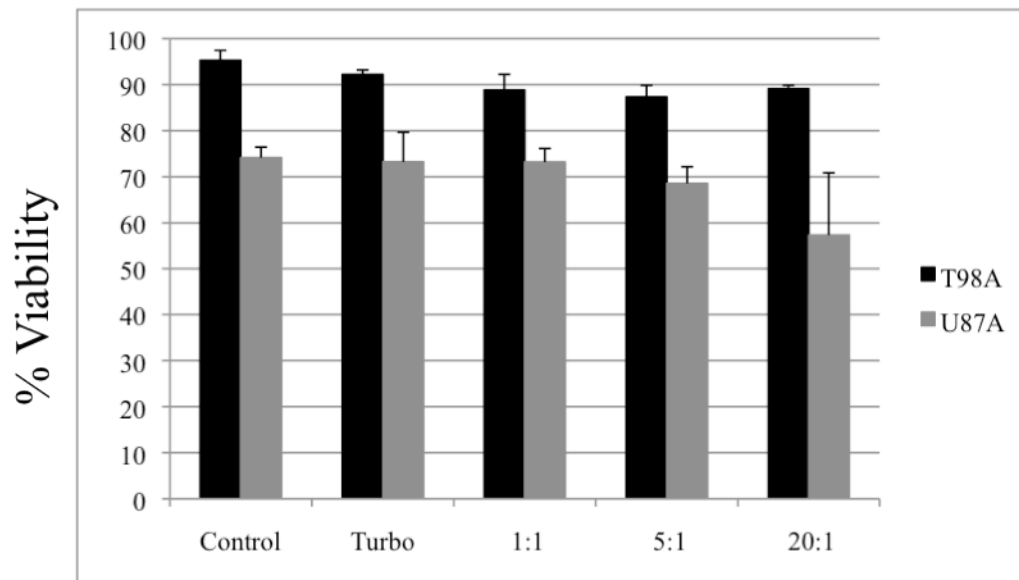**Figure 4. Trypan Blue Dye Exclusion Assay**. Trypan Blue Dye Exclusion assay results in T98A and U87A cells following transfection with folate conjugated dendrimer/EPS8pr-GFP plasmid DNA at varying concentrations (20, 5, 1 μg/1 μg) or Turbo/EPS8pr-GFP plasmid (2 μl/1μg). Assay was conducted in triplicate for each experimental parameter in both cell lines, error bars represent standard deviation (n=3).

3.4 Co-localization of G4FA-FITC With Cellular Organelle Protein Markers

Although dendrimers are widely studied as synthetic delivery systems, their exact mechanism of internalization and intracellular trafficking is not well understood. We wanted to track the internalization and trafficking dynamics of our folate-conjugated dendrimer (G4FA) using fluorescence microscopy. The fluorophore fluorescein isothiocyanate (FITC) was conjugated to dendrimer surface to facilitate visualization of our folate-conjugated dendrimer (G4FA-FITC) in these co-localization assays. First, we treated T98A and U87A cells seeded on cover slips in a 12-well plate with 5 µg G4FA-FITC/well, added to separate wells at time points starting at 24h, 6h, 3h, 1h, and 30 minutes before fixation of the whole plate in methanol, 24 hours after the first treatment. Following fixation, cells were counterstained with DAPI and antibody recognizing the early endosome protein marker, Rab5, then mounted for fluorescent microscopy (described in detail in Methods section). Co-localization of G4FA-FITC with Rab5 was apparent at 30 minutes and 1 hour (Fig.5A and 5B) as determined by fluorescent overlap between green and red channels, and became less obvious at later time points. Figure 5C includes confocal fluorescent images of the 24h incubation point from this assay in both cell lines. Figure 5C-1 is a zoom inset of the merged fluorescent confocal image of T98A in Figure 5C. The particular cells in this inset show G4FA-FITC co-localization with early endosomal marker, Rab5 at various punctate points, indicating its sub-cellular location within endosome.

We were very interested in further understanding the trafficking dynamics of the folate-conjugated dendrimer. The experiment was repeated in T98A and U87A cells as

32

described in Methods section. Primary antibodies recognizing organelle protein markers RCAS1 (Golgi) and Caveolin-1 (plasma membrane) permitted fluorescent detection of respective sub-cellular organelle locations using secondary antibody Dylight-594, to recognize bound primary antibody. Cells seeded on glass coverslips were treated with 5 ug of G4FA-FITC per well for indicated incubation times, fixed in cold methanol, counterstained with DAPI and/or antibodies recognizing cellular organelle protein markers, and mounted for fluorescent imaging. Images in Figures 5D and 5E are representative of the results found in T98A and U87A, respectively, using the protein marker for plasma membrane, Caveolin-1. Co-localization of G4FA-FITC and CAV1 was seen at 3 hour and 6 hour incubation points, indicated by yellow arrowheads. Images in Figure 5F and 5G are representative of the results found in T98A and U87A, respectively, using protein marker for Golgi apparatus, RCAS1. Co-localization of G4FA-FITC and RCAS1 was seen between 1 and 3 hours following addition of dendrimer.

Figure 5A. Fluorescent Images: T98A Treated with G4FA-FITC, Rab5 Counterstain.

T98A cells treated with G4FA-FITC for various lengths of time before fixation in cold methanol. Cells were counterstained with DAPI and primary antibody recognizing Rab5 (rabbit), then secondary antibody Dylight-594 (anti-rabbit) for recognition of bound Rab5 primary antibody. Red fluorescence= Rab5, Green= G4FA-FITC, blue= DAPI. Yellow arrowheads indicate areas of co-localization between FITC-labeled dendrimer and Rab5. All images are viewed at 630x original magnification.

Figure 5B. Fluorescent Images: U87A Treated with G4FA-FITC, Rab5 Counterstain.
U87A cells treated with G4FA-FITC for various lengths of time before fixation in cold methanol. Cells were counterstained with DAPI and primary antibody recognizing Rab5 (rabbit), then secondary antibody Dylight-594 (anti-rabbit) for recognition of Rab5 bound primary antibody. Red fluorescence= Rab5, Green= G4FA-FITC, blue= DAPI. Yellow arrowheads indicate areas of co-localization between FITC-labeled dendrimer and Rab5. All images are viewed at 630x original magnification.

35

| DAPI | G4FA-FITC | Rab5 | MERGE |

T98A:

U87A:

Figure 5C. : **Confocal Fluorescent Images: T98A/U87A Treated with G4FA-FITC 24h, Rab5 Counterstain.** Confocal fluorescent images displaying T98A and U87A cells treated with G4FA-FITC for 24h. These are the same microscope slides that were imaged in Figures 4A and 4B, described in Methods section. Individual fluorescent channels (blue=DAPI, green= G4FA-FITC, Red =Rab5) and merged images are displayed. All images are viewed at 630x original magnification.
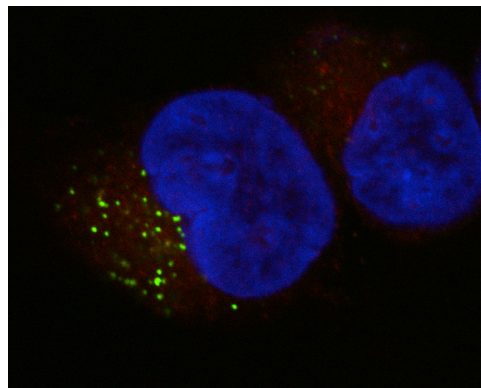
Figure 5C-1. **Confocal Fluorescent Image: Inset Zoom T98A**. Inset Zoom from the merged image of T98A above. T98A cells were incubated with G4FA-FITC for 24h, fixed

36

in methanol, counterstained with DAPI (blue), primary antibody Rab5, and secondary

antibody Dylight-594 (red) for recognition of bound primary Rab5 antibody. Image is

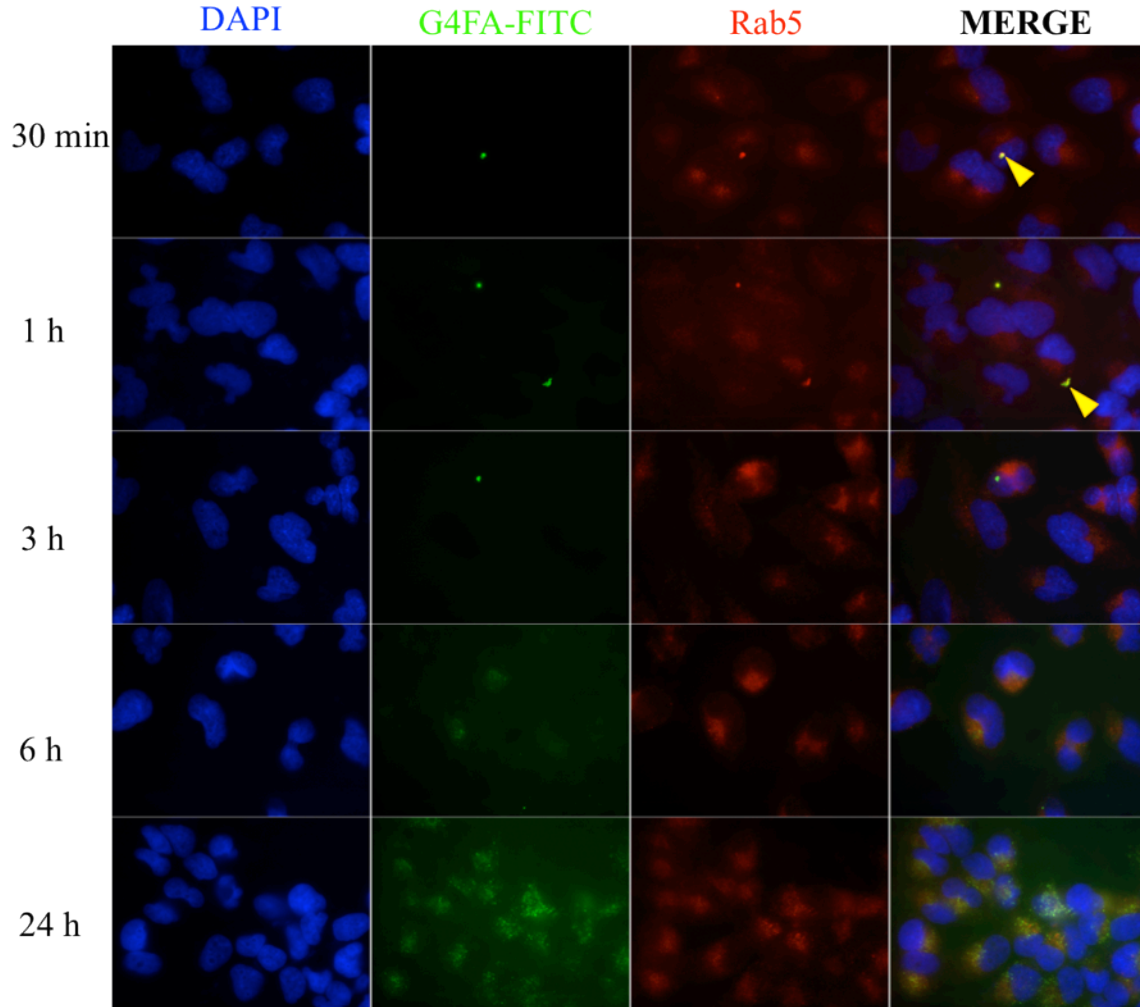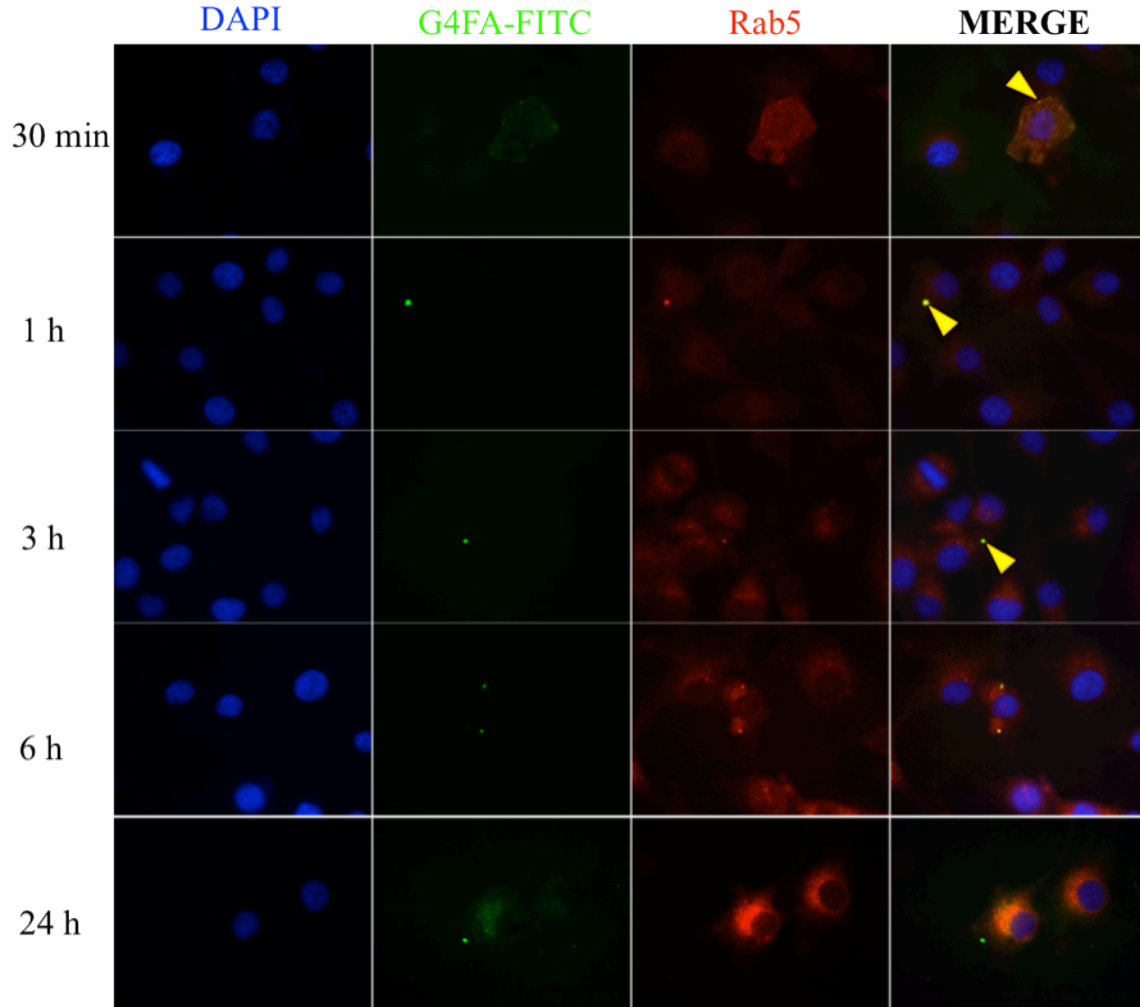zoomed from image above viewed at 630x original magnification.

Figure 5D. Fluorescent Images: T98A Treated with G4FA-FITC, CAV1

Counterstain. T98A cells treated with G4FA-FITC for various lengths of time before

fixation in cold methanol. Cells were counterstained with DAPI and primary antibody

recognizing Caveolin-1 (CAV1, rabbit), then secondary antibody Dylight-594 (anti-rabbit)

for recognition of bound CAV1 primary antibody. Red fluorescence= Caveolin-1, Green=

G4FA-FITC, blue= DAPI. Yellow arrowheads indicate areas of co-localization between

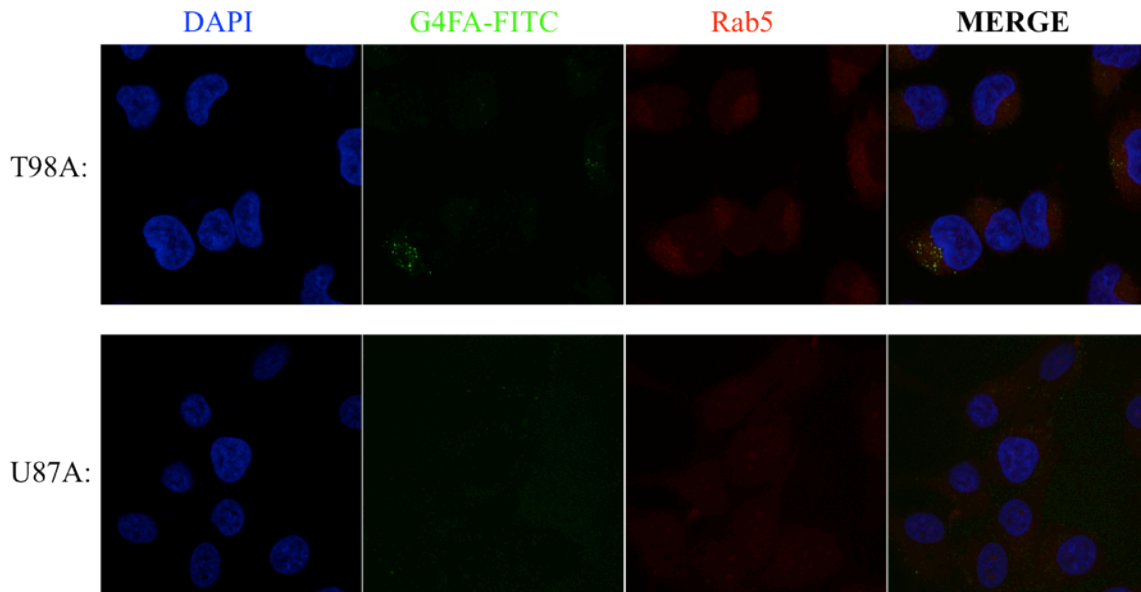FITC-labeled dendrimer and CAV1. All images are viewed at 630x original magnification.

37
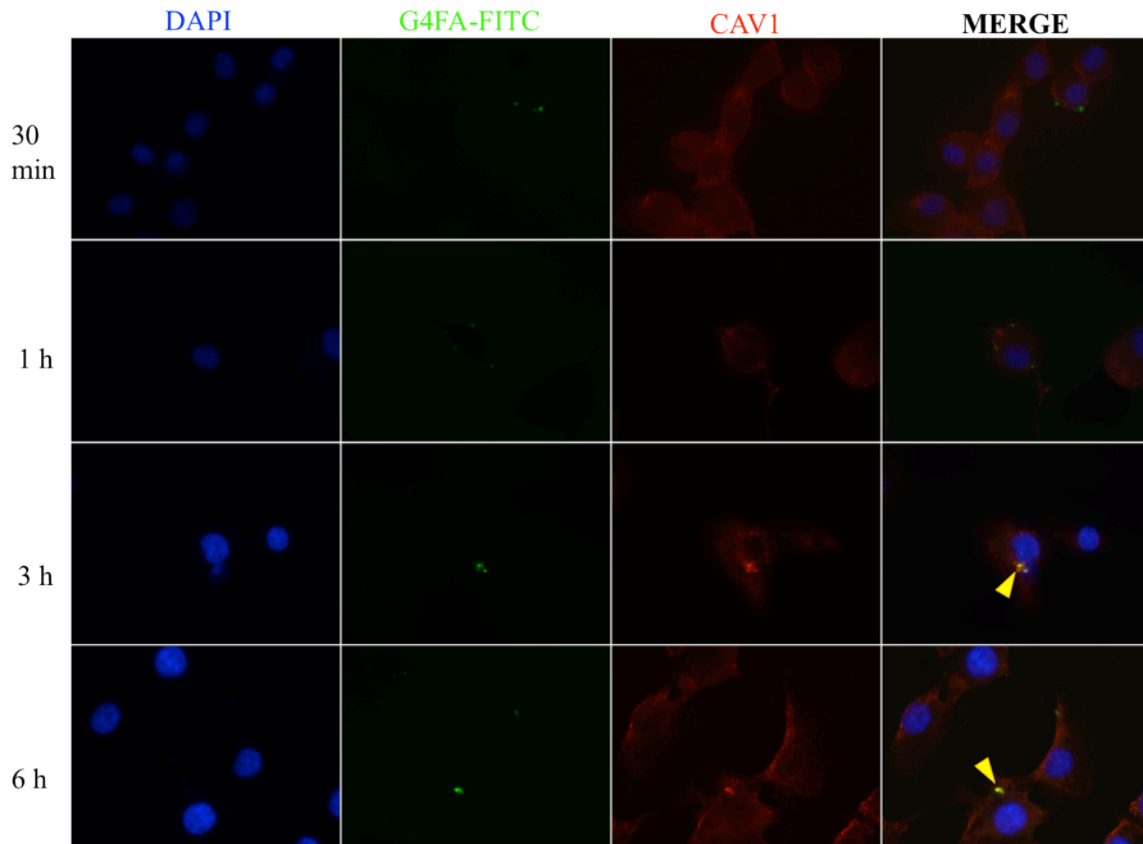
Figure 5E. Fluorescent Images: U87A Treated with G4FA-FITC, CAV1 Counterstain. U87A cells treated with G4FA-FITC for various lengths of time before fixation in cold methanol. Cells were counterstained with DAPI and primary antibody recognizing Caveolin-1 (CAV1, rabbit), then secondary antibody Dylight-594 (anti-rabbit) for recognition of CAV1 bound primary antibody. Red fluorescence= Caveolin-1, Green= G4FA-FITC, blue= DAPI. Yellow arrowheads indicate areas of co-localization between FITC-labeled dendrimer and CAV1. All images are viewed at 630x original magnification.

38
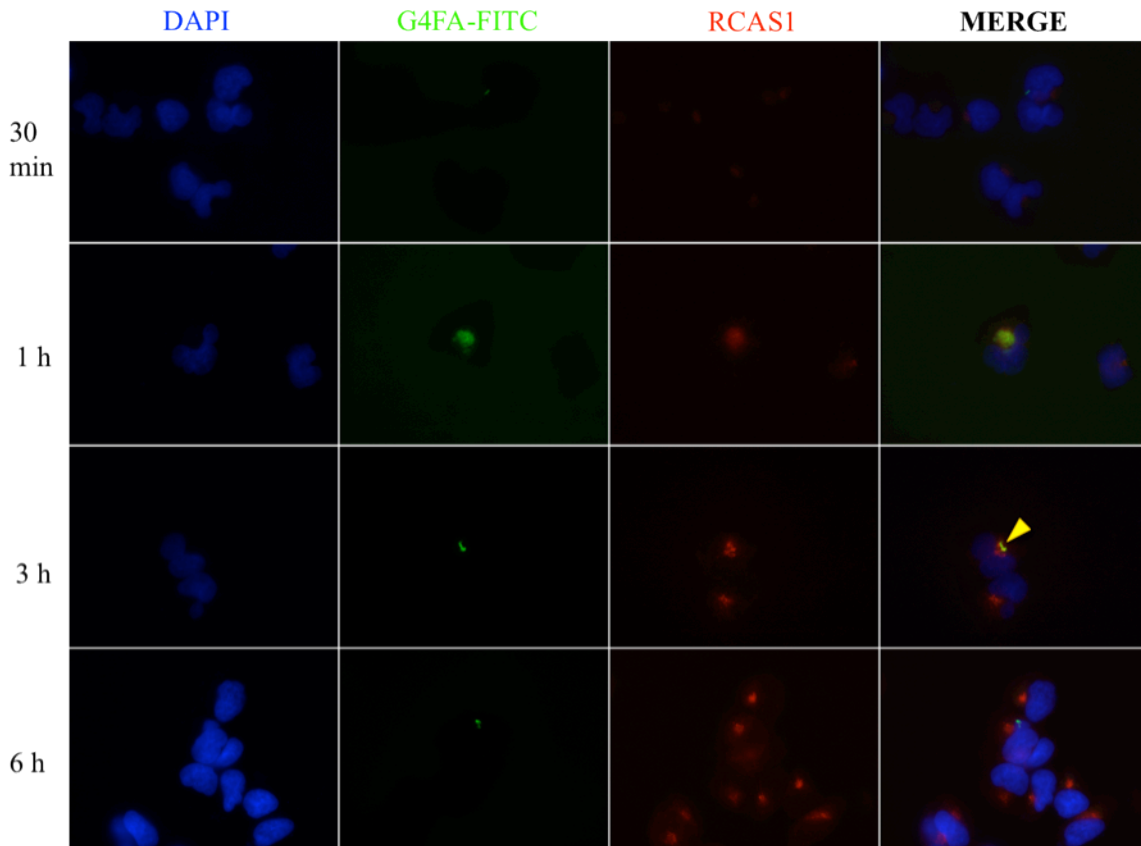
Figure 5F. Fluorescent Images: T98A Treated with G4FA-FITC, RCAS1 Counterstain. T98A cells treated with G4FA-FITC for various lengths of time before fixation in cold methanol. Cells were counterstained with DAPI and primary antibody recognizing RCAS1 (rabbit), then secondary antibody Dylight-594 (anti-rabbit) for recognition of bound RCAS1 primary antibody. Red fluorescence= RCAS1, Green= G4FA-FITC, blue= DAPI. Yellow arrowheads indicate areas of co-localization between FITC-labeled dendrimer and RCAS1. All images are viewed at 630x original magnification.
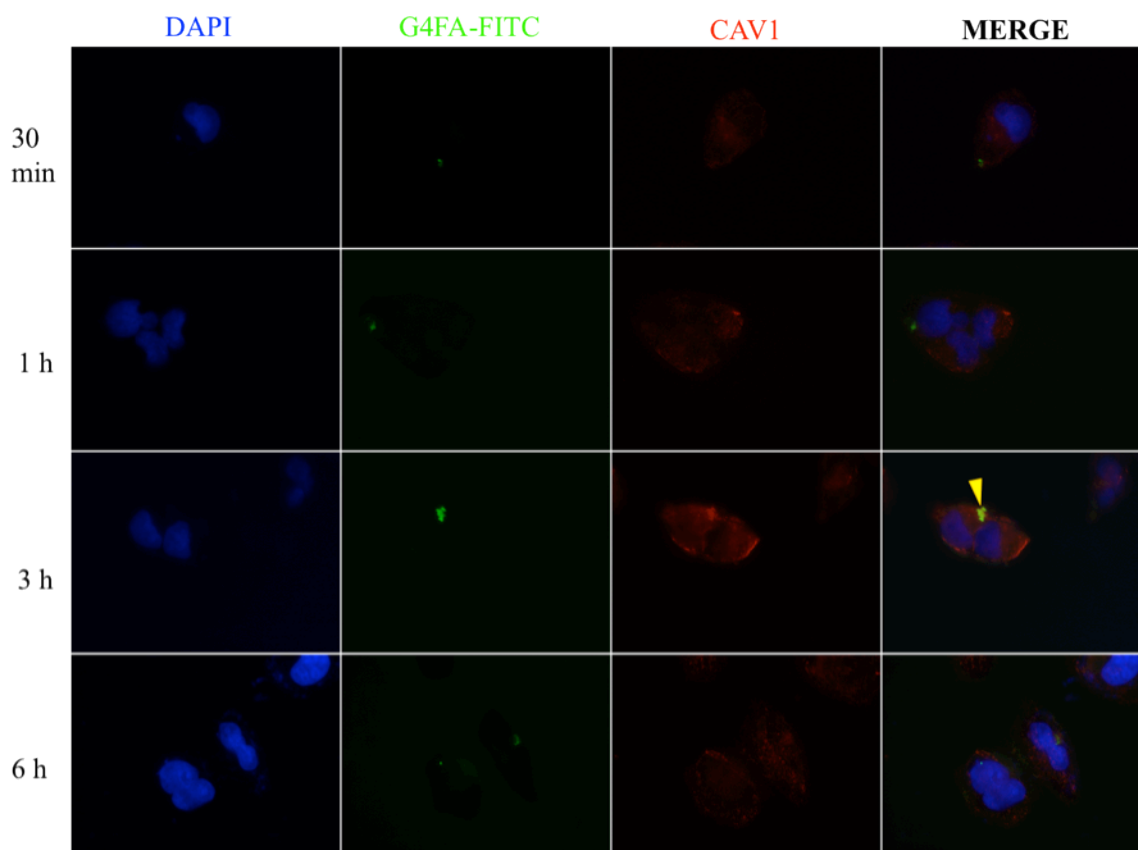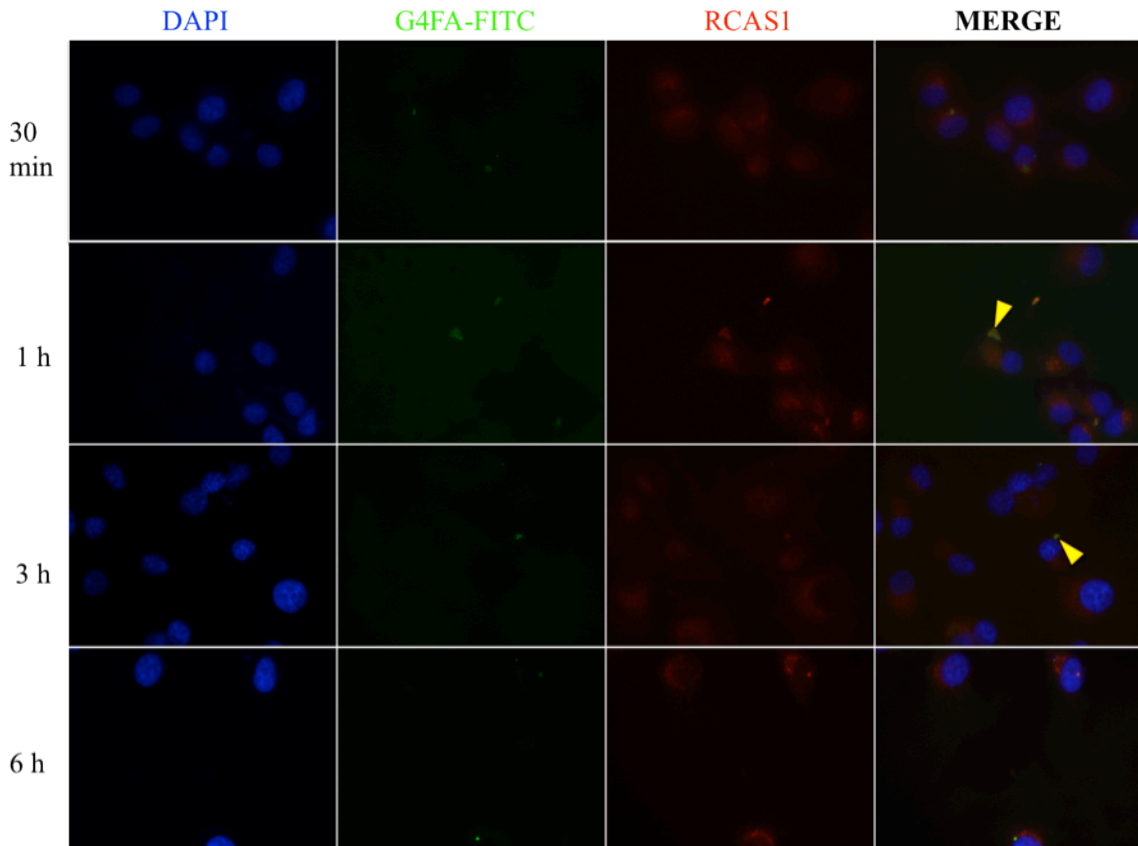
Figure 5G. Fluorescent Images: U87A Treated with G4FA-FITC, RCAS1 Counterstain. U87A cells treated with G4FA-FITC for various lengths of time before fixation in cold methanol. Cells were counterstained with DAPI and primary antibody recognizing RCAS1 (rabbit), then secondary antibody Dylight-594 (anti-rabbit) for recognition of bound RCAS1 primary antibody. Red fluorescence= RCAS1, Green= G4FA-FITC, blue= DAPI. Yellow arrowheads indicate areas of co-localization between FITC-labeled dendrimer and RCAS1. All images are viewed at 630x original magnification.

3.5 Dendrimer:Plasmid DNA Complex Dissociation

To understand the trafficking pattern of internalized dendrimer/plasmid polyplexes *in vitro*, distribution of the polyplexes in T98A cells at various time points post-transfection was assessed. A cyanine dye-labeled plasmid (Label IT® Cy3^{TM} plasmid) was employed for *in vitro* tracking of plasmid. Time course imaging and co-localization results qualitatively show the co-localization and dissociation of G4FA-FITC/cy3-labeled plasmid. Figure 6 shows fluorescent images of transfected-T98A cells at time points 30 mins, 1 hour, 3 hours, 6 hours, and 14 hours following addition of polyplexes. Results show significant co-localization of dendrimer/DNA until after 1 hour following addition of polyplexes, after which, complexes evidently begin to dissociate.

41
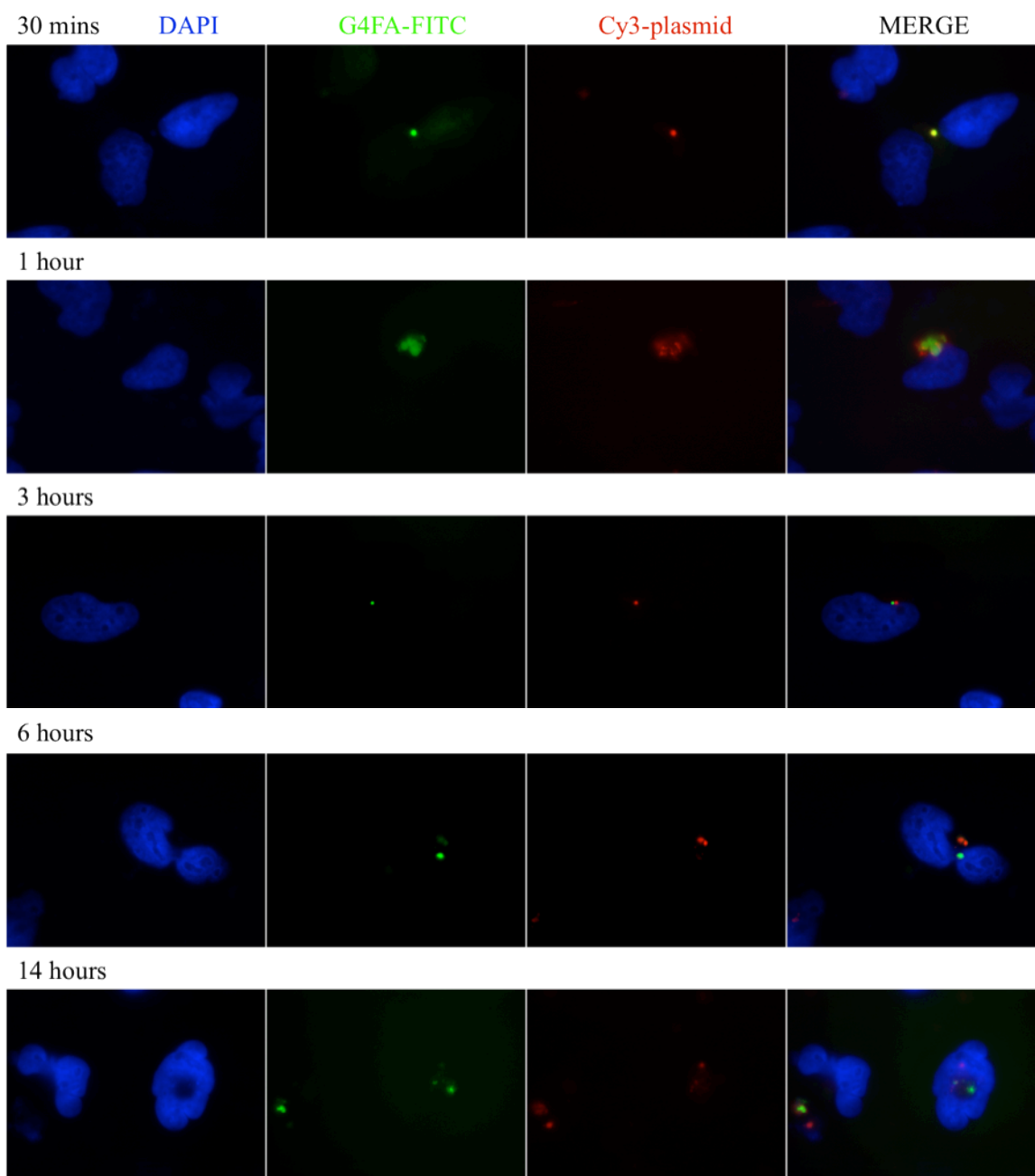
Figure 6. Dendrimer:pDNA Dissociation and Intracellular Tracking. Fluorescent

images tracking G4FA-FITC dendrimer/Cy3-labeled pDNA complex dissociation. Cells

were transfected with cy3-labeled plasmid, delivered by the FITC-labeled folate-

conjugated dendrimer (G4FA-FITC). G4FA-FITC is represented with green fluorescence.

42

Red fluorescence detects the cy3-labeled plasmid (i.e., Label IT® Cy3^{TM} plasmid) delivered by our folate-conjugated dendritic vector. Blue fluorescence detects DAPI staining of DNA. Individual fluorescent channels are shown at each time point, along with merged images to display co-localization and dissociation of dendrimer:DNA complexes within T98A cells. All images are viewed at 1000x original magnification.

43

3.6 siRNA-Mediated Down-Regulation of FOLRα

       To determine specificity of the folate-conjugated dendrimer for FOLRα, we needed to test its efficiency in cells whose FOLRα expression was significantly silenced. Knockdown of folate receptor was performed through nucleofection of T98A cells with siRNA targeting FOLRα. Negative control cells were nucleofected under the same conditions, with universal negative control siRNA (Sigma-Aldrich), which has no effect on gene expression levels. Real-time quantitative polymerase chain reaction results confirmed successful knockdown of FOLRα in T98A cells 48h post-transfection, with nearly 70% efficiency, as compared to our control siRNA-treated cells (Figure 7). siFOLRα and siNEG transfected T98A cells provided contrasting FOLRα -/+ cells, respectively, for subsequent testing of dendrimer specificity.

44
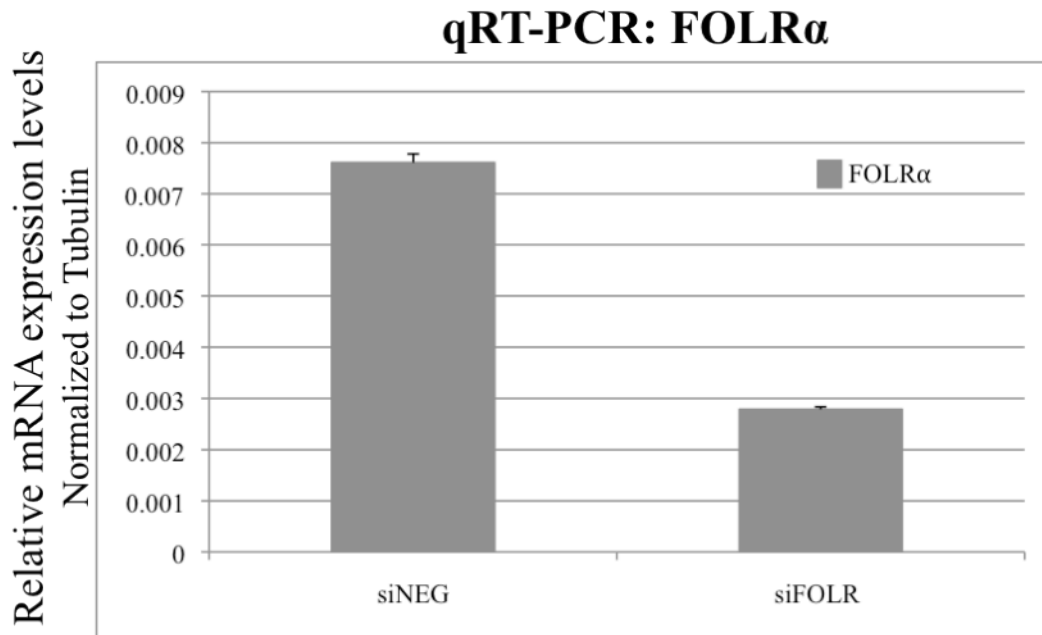
Figure 7. **qRT-PCR: Folate Receptor Alpha Knockdown.** qRT-PCR results to confirm

knockdown of Folate Receptor-α using siRNA in T98A cells. Total RNA was extracted,

reverse-transcribed, and qRT-PCR performed. The relative expression ratio is defined as

the expression levels of FOLRα to that of an internal standard, Tubulin. Assays were

carried out in triplicate; error bars represent SEM

3.7 G4FA Is Internalized By Cells In A Receptor-Dependent Manner

To test specificity of the folate-conjugated dendrimer for FOLRα positive tumor cells, we treated T98A cells from the knockdown experiment described above. siFOLRα cells and siNEG cells were treated in parallel with (or without in negative control) 5 µg of G4FA-FITC in 12-well plate. Cells were fixed in cold methanol after 1h incubation then mounted on microscope slides for study under a fluorescent microscope. As seen in Figure 8, siNEG cells, which are FOLRα-positive, showed significantly increased G4FA-FITC internalization compared to the siFOLRα cells.
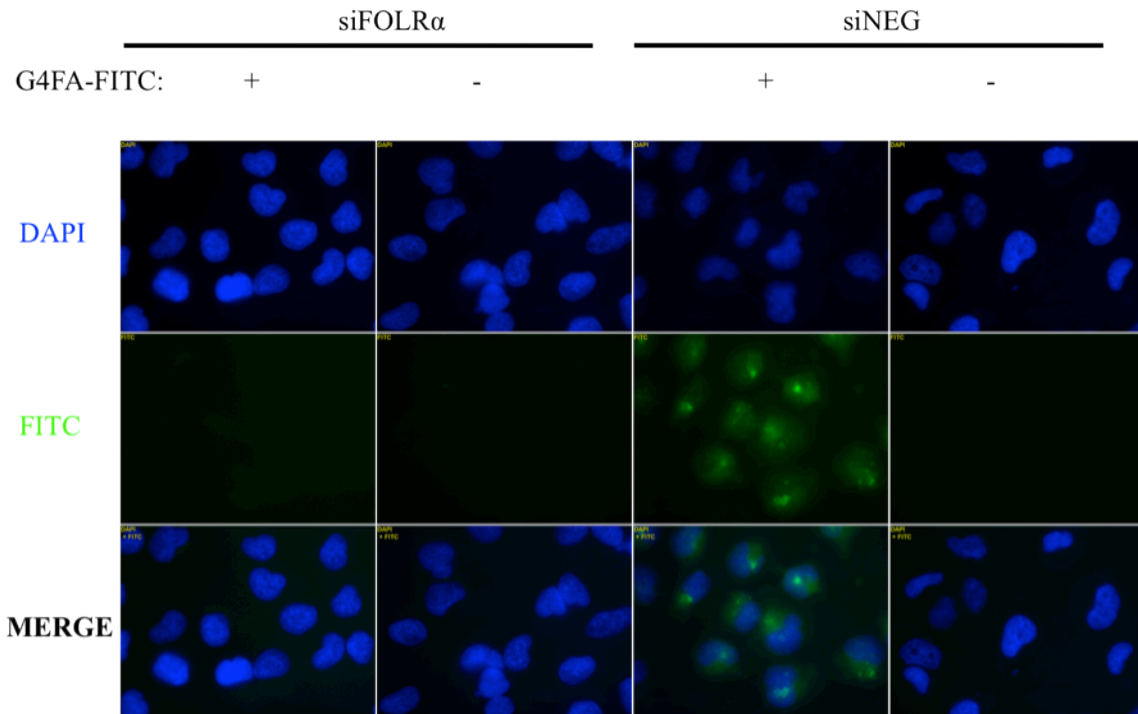
Figure 8. Fluorescent Images: siFOLRα vs. siNEG Treated With G4FA-FITC.

Fluorescent images showing T98A siFOLR and siNEG cells treated with FITC-labeled

folate-conjugated dendrimer (G4FA-FITC) or no treatment (providing a negative control

for both siRNA parameters). G4FA-FITC is represented with green fluorescence. Blue

fluorescence detects DAPI staining of DNA. Individual fluorescent channels (DAPI, FITC)

and merged images are displayed. All images are viewed at 630x original magnification.

3.8 G4FA Delivery of siRNA

Nanovectors are studied for delivery of gene therapy, of which there are several types, including plasmid DNA (pDNA), small interfering RNA (siRNA), small hairpin RNA (shRNA), microRNA (miRNA), and antisense oligonucleotides. We previously showed high transfection efficiency of plasmid DNA using the folate-conjugated dendrimer, and we wanted to explore its capabilities of delivering other gene therapeutics, like siRNA. siRNA is a potent form of RNA interference that targets specific genes or mRNA molecules to down regulate gene expression. The process is initiated by ribonuclease protein, Dicer, which binds to and cleaves dsRNA into fragments, called small interfering RNAs. Each siRNA is unwound into two strands and the guide strand is incorporated into the RNA-induced silencing complex (RISC). RISC effectively cleaves the mRNA, preventing its translation into protein and thus achieving gene silencing[24].

The capability of folate-conjugated dendrimer to deliver siRNA was tested by examining RNA interference-mediated YFP gene knockdown. Stable YFP-expressing cell lines, T98A-YFP and U87A-YFP were constructed from parental cell lines via electroporation with YFP plasmid (Amaxa nucleofection, Amaxa Biosystems). YFP-expressing cells were selected for with growth medium supplemented with G418 (1:100). Prolonged exposure to G418 effectively selected for survival of G418-resistant cells that had incorporated the YFP plasmid, which includes the neomycin resistance gene (neo). To exclude any potential interference of FITC, G4FA dendrimers were used without FITC labeling. siGFP or siNEG was used to transiently transfect YFP-expressing T98A and U87A cells (T98A-YFP, U87A-YFP). siGFP was used for knockdown of YFP expression

48

because YFP, or yellow fluorescent protein, is a designed protein variant of GFP, green fluorescent protein, and only differs in sequence by one amino acid (Thr 203→Tyr mutation). Therefore, siRNA designed to knockdown GFP expression will also effectively knockdown YFP expression. From here forward to limit confusion, I will only reference YFP. Stably transfected cell lines expressing YFP were used to determine transfection efficiency of the folate-conjugated dendrimer in delivery of siRNA targeting YFP.

Figure 9 shows Western blot analysis of protein lysates 48 hours following transfection. It is apparent that G4FA/siYFP treated T98A-YFP cells had a significant knockdown of YFP gene expression after 48 hours. The knockdown of YFP expression in U87A-YFP cells was less obvious. Figure 10 displays fluorescent images of both cell lines treated with siNEG or siYFP. Because U87A cells express FOLRα to a lesser extent than T98A, it would be expected based on our hypothesis, that T98A cells treated in the same conditions would show enhanced knockdown results when using our folate-conjugated dendrimer. Therefore, this supports the hypothesis that G4FA confers enhanced uptake in FOLRα-positive tumor cells.
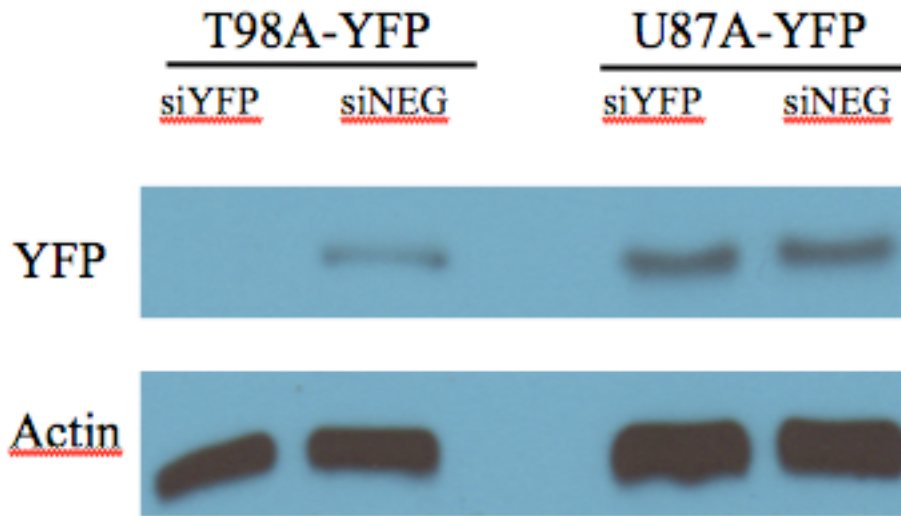
Figure 9. Western Blot Analysis of YFP Expression Following siRNA-Mediated Knockdown. Western blot analysis of total cellular protein lysates prepared from cells transfected with G4FA-FITC:siRNA (siYFP or siNEG). Total cellular protein lysates were prepared as described in Methods, and western blotted with indicated antibodies.
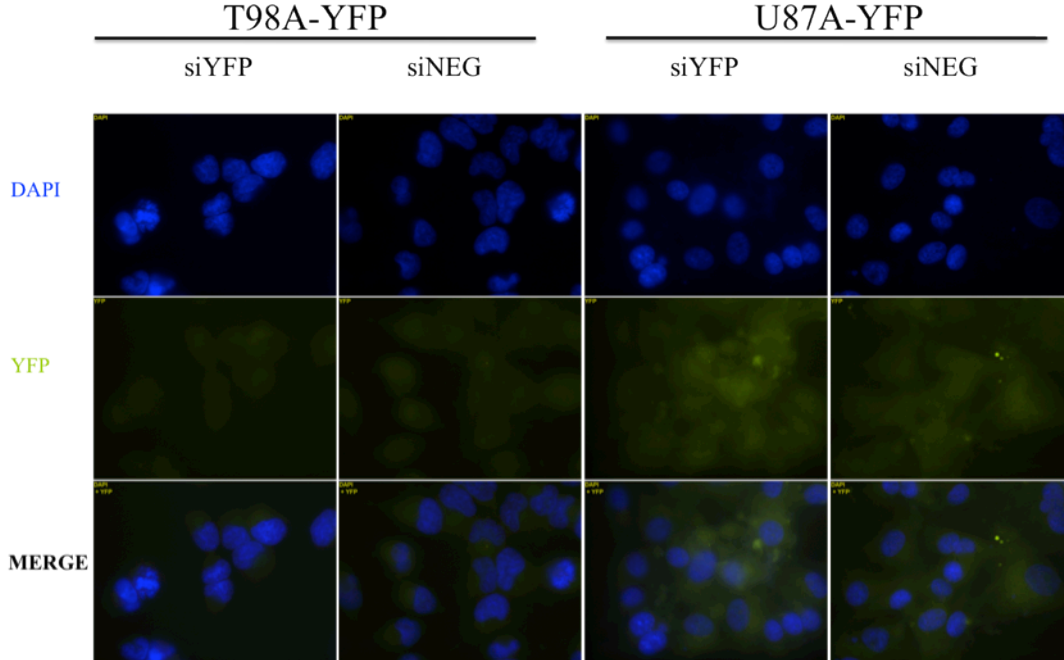
Figure 10. Fluorescent Images of YFP-expressing T98A and U87A Following siRNA-Mediated Knockdown. Fluorescent images of YFP expressing T98A and U87A cells treated with either siNEG or siYFP, 48h following transfection with G4FA for delivery of siRNA. All images are viewed at 630x original magnification.

4. Discussion

4.1 Exploiting Ligand-Receptor Relationships for Targeted Therapy

Ligand-conjugated nanoparticles have proven useful for tumor-targeted intracellular delivery through endocytosis-mediated internalization by tumor-specific receptors. The main objective in the development of targeted therapeutics is to enhance specific delivery to diseased tissue and reduce off target release. Targeted therapeutics can be designed to exploit ligand-receptor relationships for enhanced intracellular delivery with specificity for diseased tissue. Folate receptor-alpha (FOLRα) is considered tumor-specific due to its frequent overexpression in a variety of tumor types, and negligible expression levels in normal tissue[18]. This tumor-specific distribution of FOLRα expression denotes this receptor as an ideal target for nanovector-based delivery systems in targeted anticancer therapeutics.

Several research groups have developed nanoparticles conjugated to folate for use in targeted delivery systems, including metallic nanoparticles, micelles, mesoporous silica, liposomes, dendrimers, and nanotubes, among others[15]. Folate conjugates have successfully delivered imaging and therapeutic agents in malignant cells in both animal tumor models and human cancer patients, with preferential uptake seen in FOLRα-positive tumor cells[11,15,20]. Studies show folate-conjugated delivery systems exert low toxicity and show increased efficacy and pharmacokinetic behavior in comparison to non-targeted dendrimers and free pharmaceutical agents when applied *in vitro* and *in vivo*[15]. While there

52

is rising interest in research of this ligand-receptor relationship for targeted anticancer therapeutic delivery systems, studies using polyamidoamine (PAMAM) dendrimers for this purpose are rather limited. Therefore, our studies were focused on exploring folic acid conjugation to generation four PAMAM dendrimers for folate receptor-targeted delivery systems.

qRT-PCR results from glioma cell lines, T98A and U87A, and HNSCC-derived HN12 cells, confirm frequent FOLRα overexpression in a variety of tumor types (Fig.2). T98A provided a high-FOLRα expressing cell line for our studies, in contrast with U87A cells whose expression of FOLRα is markedly lower (Fig. 2). FOLRα overexpression reflects the tumors' high demand for folic acid, which is required for continual growth. Expression of FOLRα is only detectable in tumor cells and normal tissue involved in embryonic development and folate resorption[17]. Biodistribution of FOLRα in healthy tissue is limited to apical surface of polarized epithelia, which is not accessible to intravenous FOLRα-targeted therapeutics. Exploitation of this ligand-receptor relationship is a viable approach to enhance specificity of delivery systems for FOLRα-positive diseased tissue.

4.2 Dendrimer-Based Intracellular Delivery Utilizing Folic Acid Conjugation for FOLRα-Mediated Endocytosis

Dendrimers are considered the most versatile, compositionally and structurally controlled nanoscale building blocks[12]. Their low polydispersity and branched architecture with numerous surface groups and a hydrophobic core makes their structure ideal for the

53

design of highly specialized nanovectors with high loading capacity and multifunctional capabilities[1]. The ability to control and tune the chemical structure of dendrimers to design and engineer highly advanced nanovectors with specific multifunctionality makes their use exceptional in comparison to other nanovectors. Liposomes, for example, are attractive vehicles for drug delivery due to their ability to encapsulate large quantities of drug; but their therapeutic potential is compromised by a trade-off between liposome stability in circulation and liposome unloading efficiency following cellular internalization[11]. Another widely studied nanovector type, polymeric micelles, tend to disassemble below a critical concentration once diluted in the bloodstream and thereby release drug prematurely before reaching the target site when tested *in vivo*[25]. In comparison to linear polymers, dendrimers have a much higher loading capacity and their uniform branched structure allows for controlled and predictable stability and pharmacokinetic behavior. The ability to construct multifunctional dendrimers allows optimization of nanoparticle pharmacokinetics, delivery efficiency, stability, biocompatibility, and specific targeting with improved drug and/or imaging efficacy and reduced toxicity[8].

We wanted to explore folate-conjugated dendrimers (G4FA) as a synthetic vector for specific intracellular delivery. Polyamidoamine (PAMAM) dendrimers are useful for the delivery of gene therapy because their polycationic surface charge allows electrostatic interaction with the negatively charged phosphates present in nucleic acids[23]. Subsequent interaction of polyplex with anionic phospholipids and glycoproteins present on the cell membrane becomes possible with high dendrimer:DNA charge ratios, which imparts overall positive charge to the polyplex. These interactions leading to internalization of

54

polyplexes can be optimized with the addition of targeting moieties that induce active pathways for uptake. Utilizing a ligand that activates tumor-specific receptors induces receptor-mediated endocytosis of the polyplex, and effectively enhances uptake compared to passive internalization. Folic acid conjugation to generation four PAMAM dendrimer provided this ligand-receptor relationship in our studies and we wanted to explore its efficiency as a delivery system.

T98A and U87A cells were transfected with EPS8pr-GFP plasmid delivered by G4FA in varying ratios (G4FA:pDNA at 20, 5, 1 μg/1μg) in comparison with proven standard transfection methods, nucleofection and with TransIT keratinocyte transfection reagent (Mirus Bio, Madison, WI). Transfection efficiency, determined in terms of GFP expression, showed a trend of increased efficiency with increased dendrimer:DNA ratio, supporting the idea that high dendrimer:DNA charge ratios allow more efficient uptake of polyplexes (Figures 3A, 3B, 3D, 3E). U87A cells displayed GFP expression to a lesser extent (Fig. 3B) when compared to T98A (Fig. 3A) cells. This may reflect enhanced uptake of our folate-conjugated dendrimer in FOLRα over expressing cells. This led us to further studies of dendrimer uptake in FOLRα-positive vs. FOLRα-negative cells, discussed in detail later.

Figure 3C and Figure 4 show that transfection using our dendrimer has only minimal effects on cell viability, even with a high dendrimer:DNA ratio. Trypan Blue dye exclusion assay (Fig. 4), a widely accepted cell viability assay, was included to support initial cell survival data quantified by cell count and normalized with respect to the viability of the control group (Fig. 3C). The trade off between cell viability and

55

transfection efficiency is less concerning when using low-generation dendrimers because toxicity of dendrimers is dose-, generation-, and surface-charge-dependent[12]. As discussed earlier, the high dendrimer:DNA charge ratio allows for interaction with cell membrane without exerting excessive toxicity seen with higher generation dendrimers[12]. The folate-conjugated dendrimer proved to be relatively safe for efficient transfection of cells, with limited cytotoxicity seen only with high concentration of dendrimer.

Effective gene therapy vectors should be safe in terms of immunogenicity and inflammation while still ensuring intact delivery of DNA/RNA to appropriate cellular compartments. Expression of our GFP reporter gene in dendrimer-treated cells indicated that the folate-conjugated dendrimer (G4FA) is a viable approach for intracellular delivery of nucleic acids, specifically plasmid DNA, within 48 hours. G4FA dendrimer is capable of entering cells and offloading plasmid DNA, which requires nuclear localization to replicate and induce gene expression. Although dendrimers are widely studied as delivery systems, their mechanisms of internalization and intracellular trafficking are not well understood. We wanted to study how the folate-conjugated dendrimer was trafficked through the cell after observing its capabilities for nucleic acid delivery within a 48h time period.

4.3 Internalization and Intracellular Trafficking Dynamics of G4FA

To track the dendrimer's location *in vitro*, a fluorescent tag, FITC, was attached to folate-conjugated dendrimer surface. Cells were treated with G4FA-FITC and counterstained for subcellular organelle protein markers, including DAPI (DNA), Rab5

56

(endosome), RCAS1 (Golgi), and Caveolin-1 (plasma membrane) as described in the Methods section. Co-localization of G4FA-FITC with endosomal protein marker, Rab5, within 30 mins and 1 hour supports the idea that our folate-conjugated dendrimer is internalized via receptor-mediated endocytosis and then shuttled to endosomal compartments (Figures 5A and 5B). In contrast with other ligand-activated receptor-mediated endocytosis pathways, folate is essential to proliferative cell vitality, and therefore, once internalized, it is utilized rather than shuttled to lysosome for degradation. This cycling is ideal when exploiting a receptor-mediated pathway for internalization of dendrimer to ensure its stability within cells.

Variability seen with co-localization of G4FA-FITC and other cellular organelle protein markers, Caveolin-1 and RCAS1, was evident at different time points. Co-localization of G4FA-FITC with CAV1 was evident at 1h, 3h, and 6h following addition of dendrimer (Figures 5D and 5E). Caveolin-1, is a structural component of cholesterol/sphingolipid enriched plasma membrane microdomain caveolae, and is involved in vesicular trafficking, among other functions[26]. Because we believe G4FA-FITC is internalized quickly, within 30 minutes following addition, it is possible that co-localization with CAV1 at later time points represents the uptake of additional folate-conjugated dendrimers. Similarly, co-localization of G4FA-FITC with RCAS1, a type III transmembrane Golgi protein involved in vesicle formation and secretion[27], at 1 hour and 3 hours (Figures 5F and 5G) following dendrimer addition, may indicate that our dendrimer is trafficked to the Golgi following endosomal escape. Further studies are required to better

57

understand the trafficking dynamics of folate-conjugated dendrimers following internalization.

4.4 Dendrimer:DNA Complex Dissociation

Intracellular trafficking of internalized dendrimer nanovectors is not well understood. We wanted to explore the association and dissociation of dendrimer:plasmid DNA complex *in vitro* to better understand trafficking dynamics involved with dendrimer transfection of plasmid DNA. LabelIT ™ Cy3^{TM} plasmid is a plasmid control with Cy3 labeling to convey fluorescent tracking of plasmid DNA. G4FA-FITC/LabelIT ™ Cy3^{TM} plasmid in 20:1 ratio (5μg/0.25 μg in 100 μl of growth medium per well) was added to cells for various lengths of time (30 min, 1h, 3h, 6h, 14h) before fixation in methanol, counterstaining with DAPI, and mounting for fluorescent microscopy. Co-localization of G4FA-FITC with cy3 labeled plasmid was evident at early time points (1 h, 3h), after which, complexes evidently begin to dissociate (Fig. 6). This data supports our hypothesis that the folate-conjugated dendrimer is internalized rapidly, and once internalized, it is stable. Dissociation of the dendrimer:DNA complex is important for offloading of dendrimer cargo, and it would be expected to take time for the complex to traffic through the cytosol to its intended location before this can occur. Dissociation at later time points reflects this time lapse, and also lends support to evidence that the folate-conjugated dendrimer is stable within cells.

4.5 G4FA Uptake is Enhanced in FOLRα-Positive Tumor Cells

The intention of designing targeted therapeutics is to convey specificity to the delivery system for a desired site, in this case, tumor cells which express FOLRα. We used siRNA in the FOLRα-overexpressing cell line, T98A, to knockdown expression of folate receptor alpha. qRT-PCR results show that nucleofection with siRNA targeting FOLRα was successful with nearly 70% efficiency, as compared to the control that was transfected with negative control siRNA (siNEG) (Fig.7). In parallel with seeding cells for RNA isolation, transfected cells were also plated on coverslips for treatment with dendrimer. Cells were incubated with 5 μg of G4FA-FITC/well for 1 hour, then fixed in cold methanol, counterstained for DAPI, and mounted for study under fluorescent microscopy. Images in Figure 8 display a clear distinction between siFOLRα and siNEG cells treated with G4FA-FITC. FOLRα positive tumor cells, i.e. siNEG treated T98A cells, show significantly increased G4FA-FITC internalization compared to siFOLRα cells. (Fig. 8). These results indicate that our folate-conjugated dendrimer is internalized through receptor-mediated endocytosis by the FOLRα and this internalization is optimized when FOLRα is overexpressed. These data supports our hypothesis that folate-conjugation to dendrimer enhances uptake of dendrimer through FOLRα receptor-dependent mechanism.

4.6 G4FA for siRNA Delivery

Folate-conjugated dendrimer is useful in the delivery of nucleic acids, as shown previously by our studies with plasmid DNA. We wanted to explore its capabilities to deliver siRNA, to determine its potential use in siRNA-mediated gene therapy. YFP-

59

expressing T98A and U87A cells were subjected to transfection using G4FA:siRNA (either siNEG, a universal negative control, or siYFP) in 20:1 ratio (5 μg/0.25 μg per well), and were allowed to incubate for 48h before further experimentation was conducted. Western blot analysis of total cellular protein lysates from both cell lines treated with siRNA is shown in Figure 9. T98A-YFP cells showed a more efficient knockdown of YFP expression following transfection with G4FA:siYFP, as compared to U87A-YFP cells. Because T98A cells have higher expression levels of FOLRα compared to U87A, it would be expected that the folate-conjugated dendrimer would be more effective at nucleic acid delivery to T98A cells. Fluorescent images lend support to this data (Fig 10), as fluorescence of siYFP treated cells is weaker than fluorescence of siNEG treated cells. Quantification of fluorescent intensity would be beneficial when repeating these experiments. This experiment shows that G4FA is capable of delivering siRNA, with higher efficiency in FOLRα positive tumor cells.

4.7 Conclusions and Future Directions

Further research is required to better understand the intracellular trafficking of dendrimer once it is internalized by cells. It may be useful to explore *in vitro* co-localization of dendrimer with subcellular organelles in a synchronized cell population in order to decrease the amount of variability seen with prolonged dendrimer treatment. Another useful method in co-localization may be to pulse dendrimer treatment, with subsequent washing to remove treatment. This will effectively exclude the possibility of

60

uptake of additional folate-conjugated dendrimers via recycled FOLRα following initial internalization. This technique will allow intracellular tracking of the dendrimer without confusion regarding recycling of the receptor and internalization of additional polyplexes. Understanding the mechanisms of intracellular trafficking of internalized polyplexes will help researchers design biocompatible nanocarriers capable of site-specific intracellular delivery.

Folate-conjugated dendrimers have proven useful for tumor-targeted intracellular delivery through endocytosis-mediated internalization by the tumor-specific receptor, FOLRα. This could prove useful for the delivery of targeted anticancer therapy in FOLRα positive tumors. Specificity of therapeutic agents for tumor cells should decrease the unintended, off-target cytotoxicity that is often associated with standard anticancer treatment methods. G4FA is capable of efficient intracellular delivery to FOLRα positive tumor cells and provides a viable approach for tumor-targeted delivery of anticancer therapeutics, imaging agents, and gene therapy.

Abbreviations

FOLRα	Folate receptor alpha or FOLR1
FA	Folic acid (folate)
PAMAM	Polyamidoamine
FITC	Fluorescein isothiocyanate
G4	Generation four PAMAM dendrimer
G4FA	Generation four PAMAM dendrimer conjugated to folic acid
G4FA-FITC	Generation four PAMAM dendrimer conjugated to folic acid, labeled with the fluorophore, FITC
GFP	Green fluorescent protein
YFP	Yellow fluorescent protein
EPS8	Epidermal growth factor receptor pathway substrate 8
EPS8pr-GFP	Plasmid DNA containing EPS8 promoter region to drive expression of reporter gene, GFP
Cy3	Cyanine-3
LabelIT ® Cy3™	Cyanine-3 labeled plasmid
pDNA	plasmid DNA
qRT-PCR	Quantitative real-time polymerase chain reaction
siFOLRα	siRNA targeting folate receptor alpha
siNEG	siRNA universal negative control #1
siGFP	siRNA targeting green fluorescent protein
Rab5	Ras-related protein Rab-5

RCAS1	Receptor binding cancer antigen expressed on SiSo cells
CAV1	Caveolin-1
DAPI	4', 6-diamidino-2-phenylindole
FBS	Fetal bovine serum
BSA	bovine serum albumin
PBS	Phosphate buffered saline
TBS	Tris-buffered saline
HEPES	4-(2-hydroxyethyl)-1-piperazineethanesulfonic acid
EGTA	Ethylene glycol tetraacetic acid
PMSF	Phenylmethylsulfonyl fluoride
SDS-PAGE	Sodium dodecyl sulfate- polyacrylamid gel electrophoresis
TTBS	TBS with Tween®-20
SEM	Standard error of the mean

Literature Cited

1. Xu L, Zhang H, Wu Y. Dendrimer advances for the central nervous system delivery of therapeutics. *ACS Chem Neurosci*. 2014;5(1):2-13. http://dx.doi.org/10.1021/cn400182z. doi: 10.1021/cn400182z.

2. Misra R, Acharya S, Sahoo SK. Cancer nanotechnology: Application of nanotechnology in cancer therapy. *Drug Discov Today*. 2010;15(19–20):842-850. doi: http://dx.doi.org/10.1016/j.drudis.2010.08.006.

3. Kohler BA, Ward E, McCarthy BJ, et al. Annual report to the nation on the status of cancer, 1975–2007, featuring tumors of the brain and other nervous system. *Journal of the National Cancer Institute*. 2011;103(9):714-736. doi: 10.1093/jnci/djr077.

4. Bishop J. *Cancer facts : A concise oncology text.* London, GBR: CRC Press; 1999.

5. Kleihues P, Ohgaki H. Genetics of glioma progression and the definition of primary and secondary glioblastoma. *Brain Pathology*. 1997;7(4):1131-1136. doi: 10.1111/j.1750-3639.1997.tb00993.x.

6. Ohgaki H, Kleihues P. Epidemiology and etiology of gliomas. *Acta Neuropathol*. 2005;109(1):93-108. http://dx.doi.org/10.1007/s00401-005-0991-y. doi: 10.1007/s00401-005-0991-y.

7. Allen TM. Ligand-targeted therapeutics in anticancer therapy. *Nature Reviews Cancer*. 2002;2(10):750.

http://search.ebscohost.com/login.aspx?direct=true&AuthType=ip,url,cookie,uid&db=a9h&AN=7502888&site=ehost-live&scope=site.

8. Sanvicens N, Marco MP. Multifunctional nanoparticles – properties and prospects for their use in human medicine. *Trends Biotechnol*. 2008;26(8):425-433. doi: http://dx.doi.org.proxy.library.vcu.edu/10.1016/j.tibtech.2008.04.005.

9. Saad M, Garbuzenko OB, Ber E, et al. Receptor targeted polymers, dendrimers, liposomes: Which nanocarrier is the most efficient for tumor-specific treatment and imaging? *J Controlled Release*. 2008;130(2):107-114. doi: http://dx.doi.org/10.1016/j.jconrel.2008.05.024.

10. Yeo Y. *Nanoparticulate drug delivery : Systems strategies, technologies, and applications.* Somerset, NJ, USA: Wiley; 2013.

11. Lu Y, Low PS. Folate-mediated delivery of macromolecular anticancer therapeutic agents. *Adv Drug Deliv Rev*. 2012;64, Supplement(0):342-352. doi: http://dx.doi.org/10.1016/j.addr.2012.09.020.

12. Yang H, Kao WJ. Dendrimers for pharmaceutical and biomedical applications. *Journal of Biomaterials Science -- Polymer Edition*. 2006;17(1):3-19. http://search.ebscohost.com/login.aspx?direct=true&AuthType=ip,url,cookie,uid&db=a9h&AN=19064370&site=ehost-live&scope=site. doi: 10.1163/156856206774879171.

13. Medina SH, El-Sayed M. Dendrimers as carriers for delivery of chemotherapeutic agents. *Chem Rev*. 2009;109(7):3141-3157. http://dx.doi.org/10.1021/cr900174j. doi: 10.1021/cr900174j.

14. Yuan Q, Lee E, Yeudall WA, Yang H. Dendrimer-triglycine-EGF nanoparticles for tumor imaging and targeted nucleic acid and drug delivery. *Oral Oncol*. 2010;46(9):698-704. doi: http://dx.doi.org.proxy.library.vcu.edu/10.1016/j.oraloncology.2010.07.001.

15. Garcia-Bennett A, Nees M, Fadeel B. In search of the holy grail: Folate-targeted nanoparticles for cancer therapy. *Biochem Pharmacol*. 2011;81(8):976-984. doi: http://dx.doi.org.proxy.library.vcu.edu/10.1016/j.bcp.2011.01.023.

16. Lucock M. Folic acid: Nutritional biochemistry, molecular biology, and role in disease processes. *Mol Genet Metab*. 2000;71(1–2):121-138. doi: http://dx.doi.org.proxy.library.vcu.edu/10.1006/mgme.2000.3027.

17. Chen C, Ke J, Zhou XE, et al. Structural basis for molecular recognition of folic acid by folate receptors. *Nature*. 2013;500(7463):486-489. http://dx.doi.org/10.1038/nature12327.

18. Parker N, Turk MJ, Westrick E, Lewis JD, Low PS, Leamon CP. Folate receptor expression in carcinomas and normal tissues determined by a quantitative radioligand binding assay. *Anal Biochem*. 2005;338(2):284-293. doi: http://dx.doi.org.proxy.library.vcu.edu/10.1016/j.ab.2004.12.026.

19. Elnakat H, Ratnam M. Distribution, functionality and gene regulation of folate receptor isoforms: Implications in targeted therapy. *Adv Drug Deliv Rev*. 2004;56(8):1067-1084. doi: http://dx.doi.org/10.1016/j.addr.2004.01.001.

20. Low PS, Kularatne SA. Folate-targeted therapeutic and imaging agents for cancer. *Curr Opin Chem Biol*. 2009;13(3):256-262. doi: http://dx.doi.org.proxy.library.vcu.edu/10.1016/j.cbpa.2009.03.022.

66

21. Low PS, Antony AC. Folate receptor-targeted drugs for cancer and inflammatory diseases. *Adv Drug Deliv Rev*. 2004;56(8):1055-1058. doi: http://dx.doi.org/10.1016/j.addr.2004.02.003.

22. Sudimack J, Lee RJ. Targeted drug delivery via the folate receptor. *Adv Drug Deliv Rev*. 2000;41(2):147-162. doi: http://dx.doi.org.proxy.library.vcu.edu/10.1016/S0169-409X(99)00062-9.

23. Eichman JD, Bielinska AU, Kukowska-Latallo JF, Baker Jr JR. The use of PAMAM dendrimers in the efficient transfer of genetic material into cells. *Pharm Sci Technol Today*. 2000;3(7):232-245. doi: http://dx.doi.org/10.1016/S1461-5347(00)00273-X.

24. Kesharwani P, Gajbhiye V, Jain NK. A review of nanocarriers for the delivery of small interfering RNA. *Biomaterials*. 2012;33(29):7138-7150. doi: http://dx.doi.org.proxy.library.vcu.edu/10.1016/j.biomaterials.2012.06.068.

25. Tomasina J, Lheureux S, Gauduchon P, Rault S, Malzert-Fréon A. Nanocarriers for the targeted treatment of ovarian cancers. *Biomaterials*. 2013;34(4):1073-1101. doi: http://dx.doi.org.proxy.library.vcu.edu/10.1016/j.biomaterials.2012.10.055.

26. Basu Roy UK, Henkhaus RS, Loupakis F, Cremolini C, Gerner EW, Ignatenko NA. Caveolin-1 is a novel regulator of K-RAS-dependent migration in colon carcinogenesis. *International Journal of Cancer*. 2013;133(1):43-57. doi: 10.1002/ijc.28001.

27. Wolf J, Reimer TA, Schuck S, et al. Role of EBAG9 protein in coat protein complex I-dependent glycoprotein maturation and secretion processes in tumor cells. *The FASEB Journal*. 2010;24(10):4000-4019. http://www.fasebj.org/content/24/10/4000.abstract.